



**Water-responsive materials for sustainable energy applications**

Journal:	<i>Journal of Materials Chemistry A</i>
Manuscript ID	TA-REV-03-2020-002896.R1
Article Type:	Review Article
Date Submitted by the Author:	01-May-2020
Complete List of Authors:	Park, Yaewon; CUNY Advanced Science Research Center, Nanoscience Chen, Xi; CUNY Advanced Science Research Center, Nanoscience

## ARTICLE

## Water-responsive materials for sustainable energy applications

Yaewon Park<sup>a</sup> and Xi Chen<sup>a,b,c\*</sup>Received 00th January 20xx,  
Accepted 00th January 20xx

DOI: 10.1039/x0xx00000x

Water-responsive (WR) materials that mechanically change volume in response to changes in relative humidity or water/humidity gradient can generate significantly higher energy actuation over natural muscles and conventional actuators. Recent proof-of-concept demonstrations have shown the great potential of using WR materials as high performance actuator components for various energy-related applications. For example, evaporation-driven engines which are enabled by spore based WR materials directly harvest natural evaporation of water and convert it into mechanical work and electricity, highlighting the possibility of using this untapped energy source of evaporation as an additional option for clean and low-cost energy generation and storage. Despite the growing interests of these examples, researches on WR materials and their applications are still in an early stage and face multiple challenges. Namely, the fundamental mechanisms that engender material's water-responsiveness are unclear. Additionally, current systems remain difficult to scale up, and the integration of WR materials into modern engineering systems is a critical design challenge. Here, we review the current development in this emerging category of WR materials. We discuss up-to-date studies on both natural and synthetic WR materials, which include their processing, characterization methods, as well as scientific and technical challenges that can be possibly advanced by future research endeavours.

## 1. Introduction

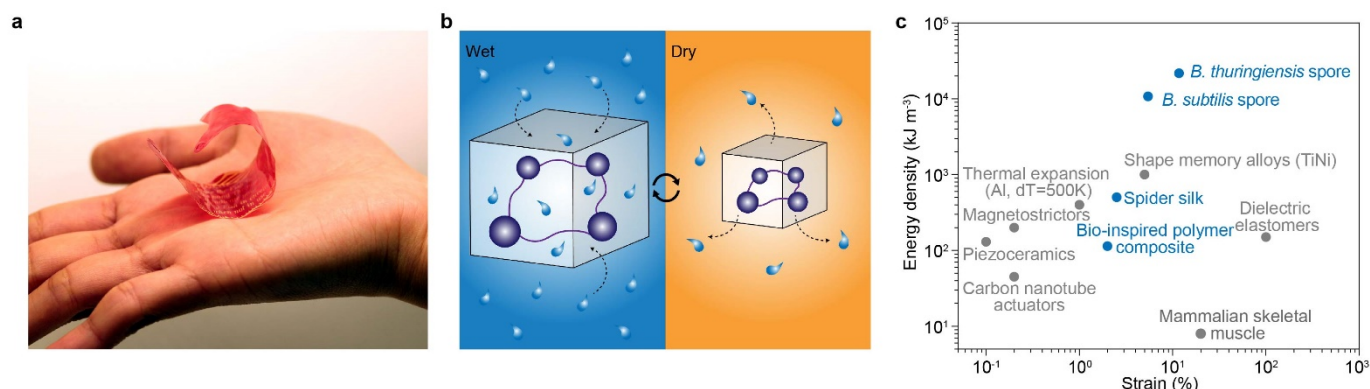


**Figure 1.** Overview of WR materials. (a) A Fortune Teller Miracle Fish automatically bends and moves when it is placed on a wet surface. (b) WR materials swell by absorbing water when the local environment is humid and shrink by desorbing water when the local environment is dry. (c) When responding to changes in RH, WR materials' actuation energy density can be significantly higher than that of conventional actuators and mammalian skeletal muscles.<sup>1</sup> Reproduced from Ref. <sup>1</sup> with permission from Nature Publishing Group.

Typically, mechanical actuators or muscles convert stimuli, such as electricity,<sup>2</sup> heat,<sup>3</sup> light,<sup>4</sup> magnetism,<sup>5</sup> or chemical reaction,<sup>6</sup> into mechanical motion. This is different from a Fortune Teller Miracle Fish that automatically bends and moves when it sits on a wet surface, for example a sweating hand (**Figure 1a**). Materials that drive these motions are usually called water-

responsive (WR) materials (also called humidity-responsive materials or water/humidity gradient responsive materials) as they can reversibly swell and shrink in response to changes in relative humidity (RH) or water/humidity gradients and convert the chemical potential of water into mechanical energy (**Figure 1b**). These materials' WR actuation can be extremely efficient and powerful. For example, wooden wedges can function as actuators as they swell when soaked with water, and they were widely used as means of splitting rocks before the modern industrialization.<sup>7</sup> While WR materials have a long history of human use as actuators, modern engineering systems have not employed this mechanism for high efficient actuation.

<sup>a</sup> Advanced Science Research Center (ASRC), City University of New York, 85 St. Nicholas Terrace, New York, NY 10031, USA

<sup>b</sup> Department of Chemical Engineering, The City College of New York, 160 Convent Avenue, New York, NY 10031, USA

<sup>c</sup> Ph.D. Program in Chemistry and Physics, The Graduate Center of City University of New York, 365 5<sup>th</sup> Avenue, New York, NY 10016, USA  
Email: xchen@gc.cuny.edu

Over the last decade, natural WR materials that exert significant actuation energy inspired the growing studies of using materials' water-responsiveness as a potentially efficient and extremely powerful actuators.<sup>1, 8-10</sup> Many examples of natural celluloses<sup>11-13</sup> and protein based structures,<sup>8, 14</sup> synthetic polymers,<sup>10, 15</sup> and composites of nanomaterials<sup>16, 17</sup> have shown remarkable WR behaviours and programmable movements, and could offer a number advantages, including high strain/stress, energy density, and efficiency, over conventional actuators driven by other stimuli (see **Table 1**). Notably, bacterial spores have demonstrated an extremely high WR actuation energy density, reaching  $\sim 20 \text{ MJ m}^{-3}$ , which is higher than the typical values reported for materials frequently used as actuators and artificial muscles (**Figure 1c**).<sup>1</sup> While WR materials' actuation could be difficult to be precisely controlled by using traditional feedback control systems (**Table 1**), their high-energy and high-efficiency actuation has recently enabled a wide range of energy-related applications, including smart structures,<sup>18, 19</sup> low power consuming actuation,<sup>20-22</sup> and electricity generation.<sup>1, 9, 23, 24</sup> For instance, using cellulose structures, architects have built weather-responsive architectural systems that can autonomously adjust their openings upon changes of local RH without using any electricity (**Figure 2a,b**).<sup>18, 19</sup> Smart textiles that open and close in response to human body's sweating facilitate comfort without adjusting the temperature of the environment (**Figure 2c,d**).<sup>25-27</sup> WR materials based soft robots can automatically and remotely operate and conduct various tasks powered by environmental RH fluctuations (**Figure 2e,f**).<sup>28-30</sup> Notably, recent pioneering researches have demonstrated the potential of using WR materials to directly and efficiently harvest energy from natural evaporation and RH fluctuations under ambient conditions.<sup>1, 9, 10, 15</sup> For example, a bioinspired polymer film of polypyrrole and polyol-borate composites flips continuously when placed on a wet surface. Taking advantage of this spontaneous WR locomotion powered by the water gradient, piezoelectric elements were attached to the film to convert its mechanical energy into electricity.<sup>10</sup> A  $\pi$ -stacked carbon nitride polymer film has also been used to demonstrate direct energy harvesting from ambient RH gradients and fluctuations. When a water droplet was placed close to the film, the minute amount of RH

fluctuations caused by the water droplet is enough to drive the film actuating and walking unidirectionally.<sup>15</sup> Furthermore, we have developed WR materials based devices, which autonomously generate piston-like linear (**Figure 2g**) and rotary motion (**Figure 2h**) when placed at air-water interfaces. These devices can directly harness energy from naturally occurring or engineered evaporation and subsequently convert it to mechanical energy or electricity,<sup>1, 9</sup> opening a new path toward the efficient harnessing of this abundant evaporation energy from water. While this energy harvesting technique is still in its early stages, theoretical studies have predicted the great potential of water as energy source.<sup>31</sup>

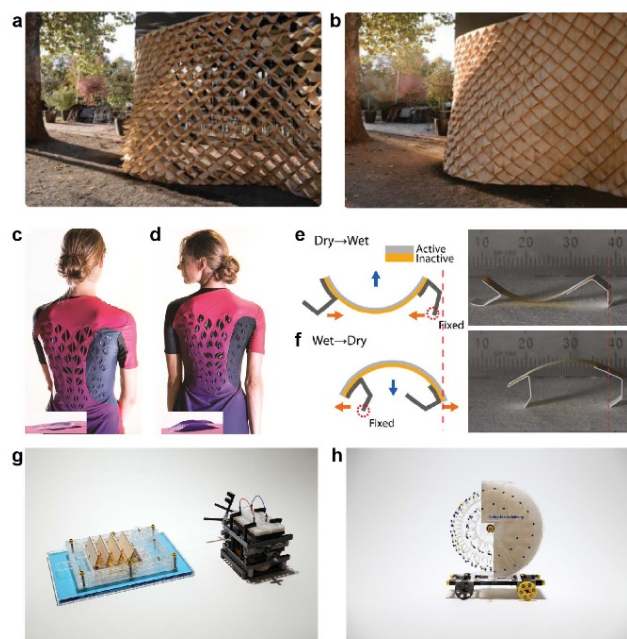


**Figure 2.** (a) Cellulose based smart architectural system opens when the local environment is dry and (b) closes when the local environment is humid.<sup>19</sup> Smart textiles with ventilation flaps (c) remain flat when the skin is dry and (d) open when the skin is sweating.<sup>27</sup> (e-f) A soft robot built with a bilayered WR structure move forward during hydration and dehydration processes.<sup>28</sup> (g) An engine generates oscillatory motions when placed above water. The oscillatory engine illuminates light emitting diodes (LEDs) when connected to an electromagnetic generator. (h) A rotary engine, powered by water evaporation from the wet paper, can continuously rotate and drive a miniature car (weighing 0.1 kg). Reproduced from Ref. <sup>19, 27, 28, 9</sup> with permission from John Wiley and Sons, The American Association for the Advancement of Science, Nature Publishing Group.

**Table 1.** Advantages and disadvantages of various stimuli-responsive materials (modified from <sup>32-34</sup>)

Stimulus type	Representative examples	Advantages	Disadvantages
Chemical potential of water	Bacterial spores Spider silk Water responsive polymers	High stress, strain, energy density, and efficiency.	Difficult to control.
Electricity	Dielectric elastomers Piezoelectric materials	Good strain, stress, and efficiency High energy density.	High voltage and fields are required.
Heat	Thermally activated shape memory alloys and shape memory polymers	High stress, strain, and energy density.	Difficult to control, low efficiency and short life cycle
Magnetism	Ferromagnetic shape memory alloys Magnetic particle/polymer composites	Good stress and strain.	Bulky magnets are required, high cost.
Chemical reaction	Mammalian skeletal muscles Chemo-responsive hydrogel	Good strain, stress, and energy density.	Complicated system.

Despite growing interests in materials' WR actuation, development of WR materials still faces challenges in scaling up, meeting efficiency expectations, and integrating them into the existing engineering systems. To this end, we intend to provide a brief overview of recent studies on WR materials. We discuss WR behaviours of newly discovered natural materials and efforts on processing natural materials and hybrid materials with natural components. We also discuss synthetic WR materials, which include their structures, water-responsiveness, and fabrication methods. To promote development of WR materials for energy-related applications, we review quantitative characterization methods that are used to evaluate the WR performance and potential for practical applications. Finally, we share our vision of remaining scientific and engineering challenges, as well as future interdisciplinary research directions that could accelerate the growth of this emerging field of WR materials.

## 2. Current Water-Responsive (WR) Materials

### 2.1. Natural WR Materials

Biological systems have developed remarkable WR materials that power their daily tasks, such as plants' dispersing or burying their seeds driven by daily RH cycles (**Figure 3a-d**). These natural WR behaviours are a consequence of their cellulose based microstructures that mechanically deform in response to RH changes.<sup>11-13, 35</sup> In addition to plants' cellulosic structures, many animal fibres and microbes were found to exhibit WR behaviours more significantly than plants.<sup>1, 8</sup> While the biological function of these animal fibres' and microbes' water-responsiveness is still not fully understood, they could potentially serve as low-cost and high-performance natural components for WR actuators and artificial muscles. In this section, we review current progresses on natural WR materials and hybrid/engineered WR materials composed of natural components.

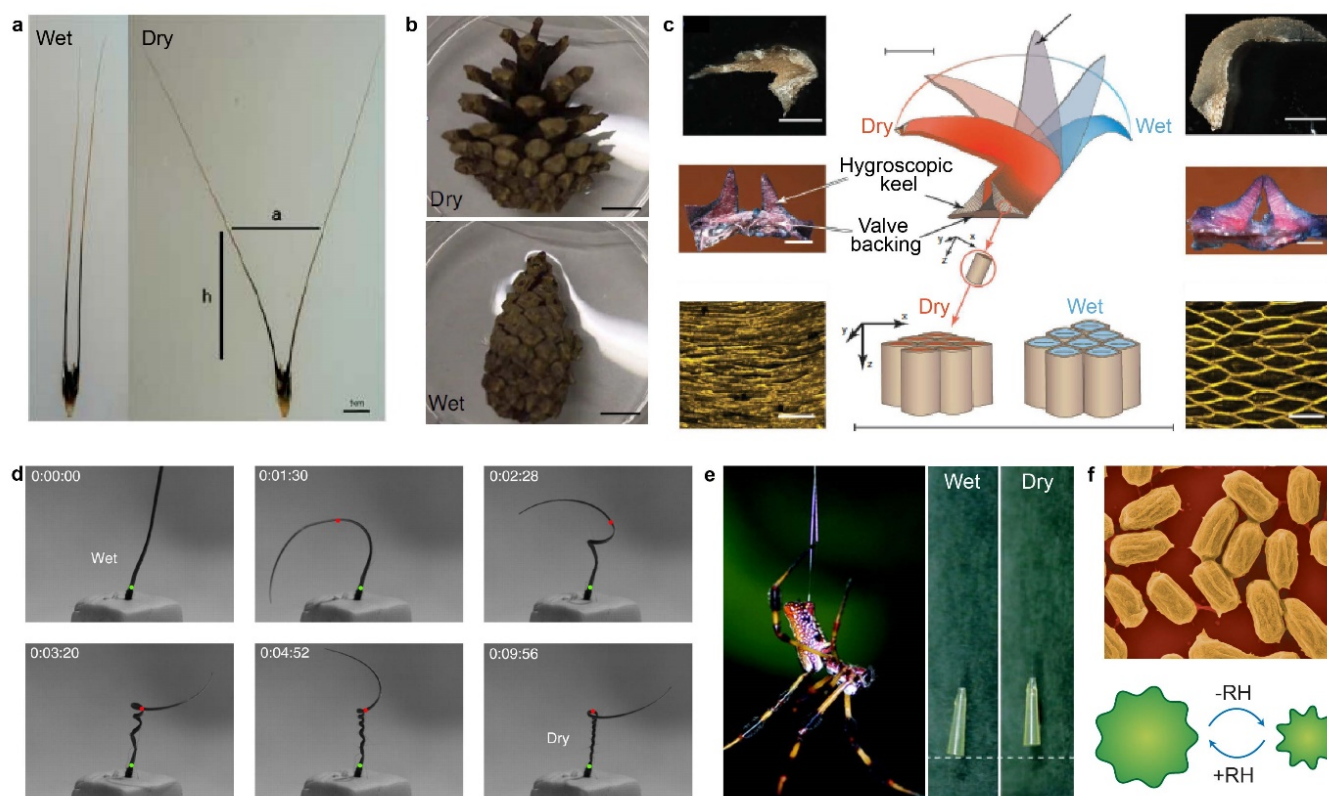


**Figure 3.** Natural WR materials. (a) Wheat awns repeatedly bend and straighten fuelled by the daily RH cycles, leading to the propulsion of its seed into the soil.<sup>12</sup> (b) The scales of pine cones open and release pine seeds when the environment is dry.<sup>44</sup> (c) Ice plant's seed capsule opens when the environment is wet due to the hygroscopic deformation of its unique keel structures.<sup>13</sup> (d) The filaree seed's awns bury the seed by drilling, as they wind and unwind with changes in ambient RH.<sup>35</sup> (e) Spider dragline silk lifts 9.5 mg of plastic weight during repeated cycles of wetting and drying.<sup>8</sup> (f) *Bacillus subtilis* spores expand and contract in response to changes in RH which can potentially generate a high amount of work.<sup>4</sup> Reproduced from Ref. <sup>12, 44, 13, 35, 8, 1</sup> with permission from The American Association for the Advancement of Science, Nature Publishing Group, The Company of Biologists, Ltd.

#### 2.1.1. Plants

The dispersal and burial of many plants' seeds rely on their WR structures' predictable mechanical motions. For example, fuelled by the daily RH cycles, wheat awns repeatedly bend and straighten, leading to the insertion of its seed into the soil (**Figure 3a**).<sup>12</sup> The scales of pine cones open and release pine

seeds when the environment is dry (**Figure 3b**),<sup>11</sup> while ice plant (*Aizoaceae*)'s keel structures open up its seed capsule when the environment is wet (**Figure 3c**).<sup>13</sup> The filaree seed drills into the soil as its awn winds and unwinds in response to fluctuations of ambient RH (**Figure 3d**).<sup>35, 36</sup>

Recent studies show that many of the plants' WR motions are controlled by bilayer structures with both active and passive layers. These bilayer structures, which usually consist of stiff crystalline cellulose microfibrils embedded in an amorphous matrix of polysaccharides, aromatic compounds, and structural proteins, can amplify the WR actuation of the active layers, but also create different types of motions, such as linear, bending, and coiling motions, to complete their vital tasks.<sup>11, 12, 37-39</sup> For instance, the bending of pine cone's scales relies on a bilayer structure that is composed of two kinds of tissues—sclerids in the outer surface and sclerenchyma fibres in the inner surface, and each surface has distinct mechanical and WR properties. When RH changes, sclerids in the outer surface deform more than sclerenchyma fibres in the inner surface, resulting in bending of the scales (**Figure 3b**).<sup>11, 38</sup> While sclerids and sclerenchyma fibre cells consist of similar amount of cellulose (~20% volume fraction), the contrast in the alignment of cellulose microfibrils differentiates their stiffness, hygroscopic expansion,<sup>11</sup> and water transport behaviours.<sup>40</sup> Wheat awns' bending motions are also controlled by a bilayer structure similar to pine cone scales, where cellulose microfibrils align in different directions per active and passive layers, leading to internal stresses to curve the entire awn structure (**Figure 3a**).<sup>12, 37</sup> Likewise, ice plant seed capsule opens up when exposed to humid environment as a result of swelling and bending of hygroscopic keels at the bottom of the seed capsule (**Figure 3c**).<sup>13</sup> Dandelion seed pappi opens and closes in response to RH changes by anisotropic swelling and shrinking of pulvinus compartments.<sup>41</sup> In addition to the bending motions, various plants use coiling motions to drive their seeds into the soil.<sup>42, 43</sup> Most of the coiling motions depend on similar bilayer structures, but hygroscopic movements of these two distinctive layers are at a tilted angle to each other. For instance, the *Geraniaceae* seeds have bilayered awns where the tilted arrangement of cellulose helices within the active inner layer leads to the coiling of awns when responding to changes in RH (**Figure 3d**).<sup>42</sup>

### 2.1.2. Animal Fibres

In addition to plants, many animal fibres exhibit outstanding water-responsiveness, such as spider silk that can shrink and expand up to ~50% in length when exposed to dry and wet environments (**Figure 3e**).<sup>8</sup> Silk produced by some spider species can generate extremely high mechanical stress and WR energy density.<sup>45,46,47</sup> For example, spider dragline silk's WR stress and energy density can reach 80 MPa and ~500 kJ m<sup>-3</sup>, respectively, surpassing that of mammalian muscles and many artificial muscles.<sup>8</sup> While it is still unclear why certain kinds of spider silks exhibit such a significant WR performance, researchers speculate that spider silk's water-responsiveness plays an important role in maintaining structural integrity of its webs and catching preys.<sup>45, 47</sup> Despite spider silks' remarkable water-responsiveness, the impracticality of spider silk farming prevents their usage in engineering applications.<sup>48</sup> In contrast, silkworm silk that has a similar primary protein structure as spider silk is readily available in large quantities.<sup>49</sup> Several groups looked into the potential of using silkworm silk as an

alternative WR material. While studies have found that silkworm silk changes length in response to continuous RH cycles, the WR stress only reaches ~20 MPa, which is much lower than that of dragline spider silk.<sup>8</sup> Other than silk fibres, camel hair, sheep hair, and goat hair also deform and recover their shapes upon immersion in water and subsequent drying process.<sup>50, 51</sup> The proposed mechanism is based on water molecules' diffusing into the amorphous regions of these fibres and the protein's intermolecular hydrogen bonds becoming disrupted, rearranging toward higher entropy states and leading to WR deformations.<sup>52, 53</sup>

### 2.1.3. Microbes

*Bacillus* spores, which we employed to build the first engines that directly harvest evaporation energy, are another type of natural WR materials.<sup>1, 9</sup> *Bacillus* spores are dormant cells formed by *Bacillus* bacteria when they are under harsh conditions, such as lacking of nutrients. Despite their dormancy, *Bacillus* spores can rapidly and powerfully expand and shrink in response to changes in RH (**Figure 3f**).<sup>1, 54, 55</sup> When local RH is alternated between 10 % and 90 %, their diameters can change by as much as ~15 % within 0.1 s.<sup>1</sup> More significantly, within 10 s, the energy exerted by *Bacillus* spores in a cycle of desorption and absorption of water is more than 20 MJ m<sup>-3</sup>, surpassing that of existing actuators and muscles (**Figure 1c**).<sup>1</sup> Later, multiple types of microbes, including wild type *Bacillus subtilis* and genetically modified *Escherichia coli* (*E. coli*) were also found to exhibit WR behaviours.<sup>27</sup> While these microbes' WR actuation are not as powerful as spores, researchers have demonstrated smart garment prototypes by printing *Bacillus subtilis* on pre-patterned latex surfaces (**Figure 2c,d**).

### 2.1.4. Hybrid/Engineered Natural WR Materials

Inspired by WR actuation of these natural examples, many natural WR materials, such as wood,<sup>18, 19</sup> papers,<sup>56</sup> natural pollen,<sup>57</sup> and cellulose nanocrystals,<sup>16</sup> have been used to develop programmable actuators that reversibly and quickly change their structures in response to RH changes. Microbes' outstanding WR properties illustrate the applicability as building blocks for ultra-high energy actuators. However, efficiently scaling up their water-responsiveness at sub-micrometre scale into a feasible engineered structure remains as a challenge. In our previously demonstrated evaporation energy harvesting devices (**Figure 1g,h**), we scaled up the spore's nanoscale WR behaviours by mixing them with adhesive and depositing the mixture on micrometre thick plastic films.<sup>9</sup> Similar to the bilayer structures found in plants, these spore based films change curvatures in response to RH changes. Patterning equally spaced spore layers on both sides of the plastic tape creates linearly expanding and contracting structures. We estimated the WR energy density of the entire strip to be approximately 17 kJ m<sup>-3</sup>, which is close to that of mammalian skeletal muscles, but these strips fail to match the possible energy density of the spore (by ~1000 times). In addition to directly using natural materials or mixing them into a matrix to form composites, some natural materials' water-responsiveness could be dramatically improved by simple

processes that alter their microstructures. Our group recently reported that regenerated *Bombyx (B.) mori* silk can be processed with simple solvent treatments to change their secondary structures (**Figure 4a-d**), which dramatically increases *B. mori* silk's WR energy density to  $1.6 \text{ MJ m}^{-3}$ , surpassing dragline spider silk's energy density (**Figure 4e**).<sup>58</sup> These examples show the possibility of using biological matters for manufacturing WR actuators potentially on an industrial scale.

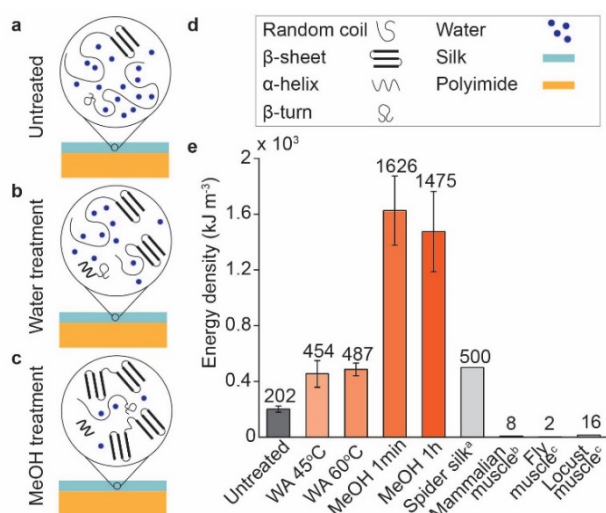


**Figure 4.** Example of regenerated biomaterials for WR actuation<sup>58</sup> (a) Regenerated *Bombyx mori (B. mori)* silk fibroin is deposited on thin polyimide substrates and subsequently treated with (b) water vapour or (c) methanol, which increases silk's  $\beta$ -sheet crystallinity. (d) Schematics of silk's microstructures, water molecules, silk and polyimide layers in (a-c). (e) WR energy density was calculated by estimating the work done by silk layer to curve the entire bilayer structure when RH is changed between 90% and 10%. WA 45°C and WA 60°C represent water vapour treatments at 45°C and 60°C, and MeOH 1min and MeOH 1h represent methanol treatments for 1 min and 1 h. Water and methanol treatments increase silk's WR actuation energy densities, surpassing that of spider silk, mammalian skeletal muscle, and muscles of black blow fly and desert locust. Reproduced with permission from Ref.<sup>58</sup> with permission from John Wiley & Sons, Inc.

## 2.2. Synthetic WR Materials

Instead of using or engineering natural WR materials, a great deal of research focus on synthetic approaches to develop WR materials. The relatively new field of synthetic WR materials has been growing rapidly. By mimicking natural structures, synthetic WR materials with programmed motions have spurred many potential applications, including soft robotics,<sup>28, 59-68, 69, 70</sup> smart textile,<sup>25, 26, 71</sup> smart windows,<sup>22, 72, 73</sup> electricity generator,<sup>10, 74-76, 23</sup> and sensors.<sup>77, 78, 79</sup> Here, we review recent progresses on synthetic WR materials, especially polymers and materials with inorganic components. We discuss their WR properties, programmable motions, as well as fabrication methods.

### 2.2.1. Polymer Based WR Materials

The redistribution of secondary bonds between polymer molecules when water molecules diffuse in or out of polymers' amorphous regions could lead to their WR behaviours.<sup>21, 82, 83</sup> This is analogous to the cyclic WR actuation of spider silk under alternating RH where disruption and reformation of the

hydrogen bonding network between silk protein molecules cause entropy-driven uncoiling/recoiling of the spider silk.<sup>52</sup>

Since hydrogels are cross-linked polymers with rich hydrophilic groups that are capable of absorbing/desorbing a large amount of water while maintaining their structural integrity, many of them exhibit WR properties. Current examples include hydrogels of sodium polyacrylate (pNaAc),<sup>80</sup> agarose,<sup>74, 76</sup> poly(ethylene glycol) (PEG),<sup>84</sup> acrylamide,<sup>16</sup> polyethylene glycol-diacrylate (PEG-DA),<sup>20, 83, 85</sup> methacrylic anhydride,<sup>86</sup> sodium alginate,<sup>87, 88</sup> polyacrylamide xerogel,<sup>82</sup> and poly(N-isopropylacrylamide)-co-acrylic acid).<sup>21</sup> WR behaviours of these hydrogels are highly dependent on their hydrophilicity and crosslinking degrees. For instance, a higher degree of swelling occurs in the region with less crosslinking, as polymer molecules have less structural restriction to move.<sup>20, 80, 87-89</sup> Thus, hydrogel's WR behaviours can be easily changed by controlling their crosslinking using a variety of methods, such as UV light irradiation<sup>20</sup> and divalent ions diffusion.<sup>80, 87, 89</sup> **Figure 5a** describes an 'ionoprinting' process where a copper electrode imprints  $\text{Cu}^{2+}$  ions into the anionic gel to locally reduce gel's water-responsiveness.<sup>80</sup> With different patterns of imprinted ions, the anionic gel's WR movement can be programmed in many ways (**Figure 5b**).<sup>80</sup> Despite programmable water-responsiveness, hydrogels' WR speeds are usually very slow. The pNaAc hydrogel in **Figure 5b** takes ~30 min to absorb water and complete its swelling.<sup>80</sup> In addition, hydrogels' mechanical strength and WR actuation stress are relatively low. Integrating inorganic materials into hydrogels appears to improve their mechanical and WR properties. Functionalized silica nanoparticle embedded hydrogels had high mechanical strength of ~110 MPa and WR stress of ~10 MPa,<sup>86</sup> but it is still a challenge for these multi-components hydrogels' mechanical and WR properties to reach that of other WR materials.

Besides hydrogels, other polymer materials, such as cellulosic papers,<sup>56, 90-92</sup> stretched nylon 6 films,<sup>93</sup> polypyrrole/polyol-borate film,<sup>10</sup>  $\pi$ -stacked carbon nitride polymer,<sup>15</sup> cellulose stearyl ester films,<sup>94</sup> polyimide-based systems<sup>95, 96</sup> have demonstrated water-responsiveness upon exposure to RH changes or water/humidity gradient. **Figure 5c** presents a spontaneous locomotion of a polypyrrole/polyol-borate film when it is placed on a moist substrate. The film consists of polypyrrole that serves as a rigid backbone and polyol-borate that can easily alter its intermolecular hydrogen bonding structures when in contact with water. When responding to water gradients, such structure exerts a high contractile stress, reaching 27 MPa.<sup>10</sup> Some hydrophobic polymers can be also modified to exhibit water responsiveness. For example, polyimide polymers that were modified by adding highly polar groups, such as ester-sulfone and carboxylic acid, showed a similar locomotion as polypyrrole/polyol-borate film when placed on moist surfaces.<sup>95</sup> Certain shape-memory polymers (SMPs), including polyester copolymer,<sup>97</sup> poly(lactic-co-glycolic acid),<sup>98</sup> poly(ethylene glycol),<sup>99, 100</sup> polyurethane,<sup>101</sup> poly(vinyl alcohol),<sup>102, 103</sup> epoxy,<sup>104</sup> agarose/polyacrylamide,<sup>105</sup> were also programmed to be WR. These SMPs usually require

“programming steps” which involves deforming the polymer at high temperature above its glass transition temperature ( $T_g$ ) to program a temporary shape that could be maintained at a lower temperature. As water molecules penetrate into the SMPs, water disrupts physical crosslinks (usually hydrogen bonding), and causes the SMPs to return to their permanent shapes.<sup>84, 97-105</sup> Many of SMPs are biocompatible and can actuate upon immersion in water at an elevated temperature,<sup>100, 102, 104</sup> which makes them great candidates for biomedical applications, including drug delivery<sup>98, 101, 102</sup> and cell scaffolds.<sup>97</sup> Recent research found that integrating cellulose nanofibres into

polyurethane matrix dramatically decreases its responsive time to less than 1 min, which is possibly due to a faster water absorption facilitated by these cellulose nanofibres.<sup>101</sup> Notably, many polymers' WR movements can be extremely rapid. For example, the  $\pi$ -stacked carbon nitride polymer can curl up within  $\sim 50$  ms when the irradiation of ultraviolet light locally heats samples and disrupts the equilibrium state.<sup>15</sup> Hydrophobic nanoparticle coated cellulose stearoyl ester films starts bending within 1 s when put on moist surfaces.<sup>94</sup>

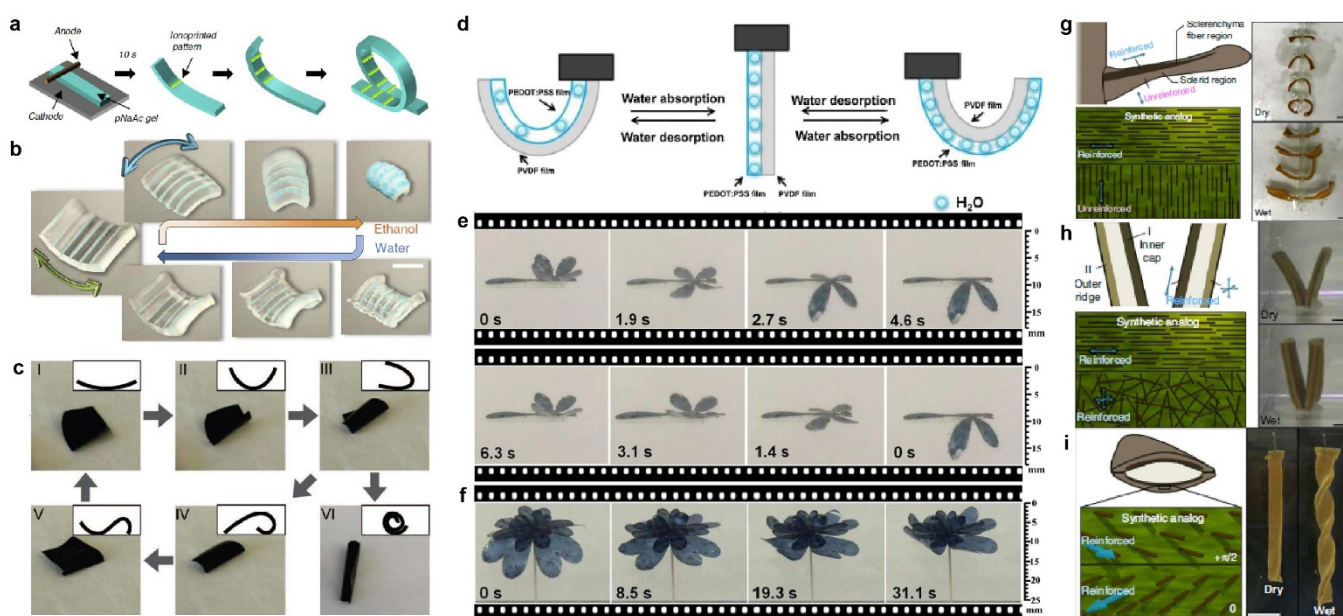


**Figure 5.** Polymer based synthetic WR materials. (a) Crosslinking gradient within a hydrogel is created by the ‘ionoprinting’ process where a copper electrode imprints  $\text{Cu}^{2+}$  ions into the anionic gel with application of electric potential at the electrode. (b) Stresses induced by the lines ionoprinted with a copper wire anode fold a 3D gel coil. This 3D shape is conserved when the gel shrinks in ethanol.<sup>80</sup> (c) Water gradient across poly(pyrrole)/poly(vinyl-borate) film leads to spontaneous WR locomotion when in contact with wet surface.<sup>40</sup> (d) Bending of bilayer structures of PEDOT:PSS/PVDF film upon RH changes was induced by differential swelling between hygroscopic PEDOT:PSS layer and inert PVDF film. (e) Flying dragon fly and (f) blooming flower were assembled with WR PEDOT:PSS/PVDF.<sup>84</sup> Plant’s bilayer-inspired design of polymer composite for predetermined WR actuation. Magnetic particles were aligned within the polymer matrix to mimic (g) pine cone’s and (h) wheat awn’s bending motion and (i) orchid tree seed pod’s twisting motion.<sup>44</sup> Reproduced from ref <sup>80, 10, 81, 44</sup> with permission from Nature Publishing Group, The American Association for the Advancement of Science and Elsevier.

Polymer based WR materials are amenable to various established methods to change their chemical and mechanical structures to control their water-responsiveness, thus yielding advantages in programming motions for different applications.<sup>16, 28, 44, 61, 65-68, 76, 81, 87, 106-111</sup> Hydrophilic groups (e.g.  $-\text{OH}$ ,  $-\text{NH}$ ,  $-\text{O}-$ ) on polymer chains can affect the bulk polymer’s water absorption behaviours. It has been demonstrated that a higher degree of substitution of hydroxyl with stearoyl esters resulted in less curling of the cellulose stearoyl ester film in response to alternating RH.<sup>94</sup> In addition to these simple methods that alter polymer’s WR properties, many researchers have resorted to biomimetic approaches to achieve various types of WR motions. Inspired by natural bilayer structures that facilitate bending, twisting, and coiling motions,<sup>11, 12, 37, 38</sup> polymeric materials are constructed with various bilayer structures where individual layers swell in different degrees upon RH changes, leading to varied motions as a result of inhomogeneous internal stresses.<sup>28, 61, 65-68, 76, 81, 87, 106-112</sup> **Figure 5d** shows a schematic of WR bending of a poly(3,4-ethylenedioxythiophene):

sulfonate/poly(vinylidene fluoride) (PEDOT:PSS/PVDF) bilayer structure where the PEDOT:PSS layer has exceptional water-responsiveness whereas PVDF is inert to RH changes.<sup>81</sup> Using this bilayer structure, RH-driven dragonfly wings that bend during hydration ( $\sim 4.6$  s) and dehydration ( $\sim 6.3$  s) (**Figure 5e**) and an artificial flower which blooms in response to RH changes (**Figure 5f**) were demonstrated.<sup>81</sup> Similarly, bilayer structures with electrospun poly(ethylene oxide) (PEO) nanofibres on a stretched poly(dimethylsiloxane) (PDMS) substrate respond to RH changes within 1-10 s, mimicking the rapid closure of the Venus flytrap leaf.<sup>109</sup> In another research, biomimetic structures with different alumina platelets aligned within gelatin polymer matrix achieved bending and twisting motions, emulating WR motions of pine cones, wheat awns, and orchid tree seed pods (**Figure 5g-i**).<sup>44</sup> In addition, liquid crystalline (LC) polymers demonstrated a similar programmability of WR actuation.<sup>113-115</sup> Typically, LC polymer consists of a network of rigid mesogens and flexible linker regions. These WR LC polymers absorb water and swell along the direction perpendicular to the alignment of mesogens. By controlling the mesogens’ alignment, various

mechanical motions, including bending, folding, and curling, were successfully programmed.<sup>113-115</sup>

The bilayer structure is not always necessary to program polymers' WR properties as the addition of stiff fillers within polymer system alone can induce inhomogeneous stresses that results in different kinds of movements. For example, 3D printed composites composed of stiff cellulose fibrils embedded in soft acrylamide achieved complicated movements similar to the blooming of flowers<sup>16</sup> and glass fibres attached to a poly(N,N-dimethylacrylamide) hydrogel base simulated the WR opening and closing of dandelion pappi.<sup>41</sup> Using a similar concept, cellulose nanocrystals (CNCs) were integrated into liquid crystalline structures to improve their water-

responsiveness and achieve designed deformation.<sup>116, 117</sup> Moreover, integrating nanopores that promote water transport inside polymers can also be used to program various WR motions.<sup>25, 71, 118</sup> For example, by taking advantage of inherent nanoscale molecular channels within perfluorosulfonic acid ionomer (PFSA) films, researchers fabricated WR actuators with both bending and helical actuations.<sup>25, 71</sup> In a similar fashion, an engineered protein, Consensus Tetratricopeptide Repeat protein (CTPR18), forms nanochannels that affect the CTPR18 film's WR behaviours with programmed bending and twisting.<sup>118</sup> By decreasing the length of the nanochannels by half, responsive time of the CTPR18 film was reduced by ten times.

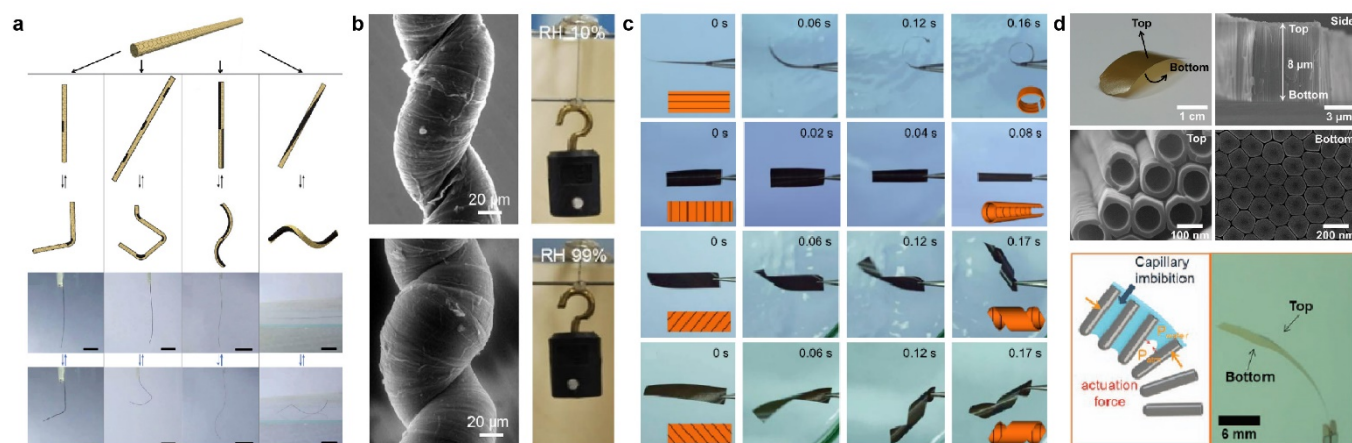


**Figure 6.** 1D and 2D nanomaterials based synthetic WR materials. (a) Graphene oxide fibres with selectively reduced regions by laser irradiation generate various motions in response to RH changes.<sup>29</sup> (b) Twisted CNT yarns with a polymer (poly(diallyldimethylammonium) chloride) sheath expand when RH is low and contract when RH is high in linear direction.<sup>119</sup> (c) Bilayered actuators consisting of aligned CNTs on a GO substrate programs bending and twisting motions.<sup>120</sup> (d) A film of with free standing titanium oxide nanocapillaries bends by capillary forces generated in response to RH changes.<sup>121</sup> Reproduced from Ref 29,<sup>119, 120, 121</sup> with permission from Angewandte Chemie International Edition, The American Association for the Advancement of Science, American Chemical Society, and Nature Publishing Group.

### 2.2.2. WR Materials with Inorganic Components

1 dimensional (1D) and 2 dimensional (2D) based materials have been extensively investigated for mechanical actuation in response to thermal and electrochemical stimuli.<sup>122, 123</sup> Recently, they have demonstrated a great potential for developing WR actuators.<sup>17, 22, 124-126</sup> For example, graphene oxide (GO) 2D materials curve rapidly when put on a wet surface.<sup>69, 79, 127</sup> Bilayer films comprising reduced graphene oxide (rGO)/GO bilayers generate bending motions upon alternating RH, because GO has more hydrophilic groups such as hydroxyl, epoxy and carboxyl groups than rGO, making GO layers more prone to swell.<sup>23, 70, 128, 129</sup> In addition, bilayer structures of GO on hydrophobic polymer films, such as polyvinylidene fluoride,<sup>130</sup> polydimethylsiloxane<sup>131</sup> and polypyrrole,<sup>132</sup> have demonstrated rapid WR actuation. In another research, hydrophilic groups of selective regions of GO fibres were reduced by laser beam irradiation.<sup>29</sup> Careful selection of laser-induced reduction of GO fibres leads to predetermined motions such as partial folding, twisting, and bending as GO absorbs more water than rGO (**Figure 6a**). Recent research also uses CNT to develop WR materials, which show forceful and fast WR actuation.<sup>17, 22, 119, 133, 134</sup> Notably, when expanding and contracting in response to RH cycles, CNT hybrid twisted yarns exhibit a large tensile stroke up to 78% and an

extremely high energy density of  $1.8 \text{ MJ m}^{-3}$  which is higher than actuation energy density of conventional nickel titanium (NiTi) shape memory alloy ( $1 \text{ MJ m}^{-3}$ ) (**Figure 6b**).<sup>119</sup> Since aligned CNTs tend to induce lateral swelling, the orientation of CNTs coated on the GO substrate directly programs the CNT/GO films' movement that is analogous to plants' WR twisting (**Figure 6c**).<sup>120</sup> The WR speed for these CNT/GO films was as fast as 0.08 s which is comparable to the snapping speed of the Venus flytrap.

In addition to 1D and 2D WR based materials, materials with other inorganic components have also been engineered to exhibit water-responsiveness. For example, some hydrophilic ceramics and metals with nano-scale porous structures, including titanium oxides,<sup>121, 135</sup> silica,<sup>136</sup> gold,<sup>137</sup> can actuate strongly due to water capillarity. When responding to changes in RH, a titanium oxide film with well aligned nanocapillaries exhibits extremely high energy density of  $1.25 \text{ MJ m}^{-3}$  (**Figure 6d**).<sup>121</sup> A nanoporous gold film prepared by electrochemical dealloying process also shows dramatic water-responsiveness and its energy density reaches  $0.15 \text{ MJ m}^{-3}$ .<sup>137</sup> Interestingly, some metal-organic frameworks (MOFs), an important class of inorganic-organic hybrid materials with highly nanoporous structures, have shown WR properties.<sup>138-140</sup> For example, a



specific type of MOF crystal, MIL-88B-Fe that is synthesized in dimethylformamide (DMF), changes its unit cell's volume by almost 25% upon dispersing in water.<sup>138</sup> Such WR behaviours of MOF crystals have been mixed with the poly(vinylidene fluoride) polymer to achieve macroscopic WR actuation, whose motion can be programmed by patterning the MOF/polymer composites using chemical etching.<sup>139, 140</sup>

### 2.3. Actuation performance comparison of natural and synthetic WR materials

Despite the recent demonstrations of synthetic WR materials, to the best of our knowledge, their performance is still not as good as natural materials, and the design criteria are not well established. We summarize and compare reported values of WR strain, stress, energy density, and response time of current natural and synthetic WR materials in **Table 2**. While some synthetic materials, such as CNT hybrid yarn<sup>119</sup> and titanium oxide films,<sup>121</sup> exhibited relatively high WR energy density, most of synthetic WR materials' performance is still far below that of natural examples such as bacterial spores.<sup>1</sup>

Table 2. Representative examples of WR materials with promising actuation properties for energy related applications

WR material type	Material description	WR actuation motion	Strain (%)	Stress (MPa)	Energy density (kJ m <sup>-3</sup> )	Response time (s)	Ref
Natural	Spruce ( <i>Picea abies</i> ) wood	Linear	8~9	1.2	48~54*	~360	141
	Spider silk	Linear	2.5	~50	500	2-3	8
	Bacterial spore	Linear	11.7	-	21300	0.1	1
	Rat tail tendon	Linear	~5	~100	2500*	-	142
Engineered natural	Regenerated silk film	Bending	2	14	1626	-	58
	Twisted degummed silk fibre	Linear	3.3	12.5	172	67	26
Synthetic polymer	Photoactive dopant/agarose hybrid film	Bending	-	-	7.4**	1.2	75
	Bioinspired polymer (PEE-PPy)	Bending	2.5	27	114	0.1	10
	Nylon 6 film	Bending	5	2.5	22	<30	93
	Functionalized silica embedded hydrogel fibre	Linear	12.5	~10	625*	-	86
Synthetic inorganic	CNT hybrid yarn	Linear	14.3	22.5	1800	<6	119
	Graphene fibre	Rotational	-	-	~520**	3.2	124
	Titanium oxide film with nanocapillaries	Bending	~0.9	-	1250	<10	121
	Nanoporous gold alloy	Linear	0.52	19	150	120-180	137

\*estimated based on the reported strain and stress values\*\* estimated based on the reported power density and response time

### 2.4. Fabrication Methods

Low cost and industrial processability make synthetic WR materials, especially polymer based WR materials, promising for large-scale manufacturing. Currently, constructing a bilayer structure that contains active and passive layers is one of the most popular strategies in imparting various WR motions for applications.<sup>28, 61, 65, 67, 68, 76, 81, 87, 106-111</sup> In these bilayer structures, active layers mostly consisting of hydrophilic components, such as cellulose papers,<sup>65, 73</sup> polyethylene oxide (PEO),<sup>28, 109</sup> sodium alginate,<sup>62, 87</sup> and chitosan,<sup>68</sup> are adhered onto passive layers usually consisting of hydrophobic components, such as polyvinyl chloride (PVC),<sup>106</sup> polypropylene (PP),<sup>65, 73, 146, 147</sup> polyimide (PI),<sup>28, 148</sup> polyvinylidene fluoride (PVDF),<sup>81, 87</sup> and polytetrafluoroethylene (PTFE).<sup>62, 108</sup> To fabricate these bilayer structures, one of the most widely used methods is solvent-casting, where solution with active components is poured onto passive substrates and subsequently allowed for drying to form films (**Figure 7a**). Using the solvent-casting method, stiff fillers

can be easily incorporated into a polymer matrix to program multiple WR motions as described in the previous sections. Examples include casting agarose solution onto aligned glass fibre fillers<sup>76</sup> and embedding magnetic field aligned metallic particles in gelatin matrix (**Figure 5d-f**).<sup>44</sup> Despite the simplicity of the traditional solvent-casting method, it is usually difficult to control the uniformity of these casted films. Spin coating, another facile method to produce highly repeatable and uniform films, was used to fabricate WR bilayer structures. As shown in **Figure 7b**, a PEDOT:PSS/PDMS bilayer WR actuator with a well-controlled homogeneous and reproducible thickness was fabricated by spin coating.<sup>67</sup> To fabricate this bilayer structure, a passive PDMS layer was first spin coated onto a silicon wafer, followed by air plasma treatment to enhance the adhesion between the PDMS layer and the PEDOT:PSS layer. PEDOT:PSS was then spin coated on the top of plasma-treated PDMS substrate. Finally, the PEDOT:PSS/PDMS bilayer WR actuator was laser cut into a predetermined shape and peeled off from the silicon substrate.<sup>67</sup>

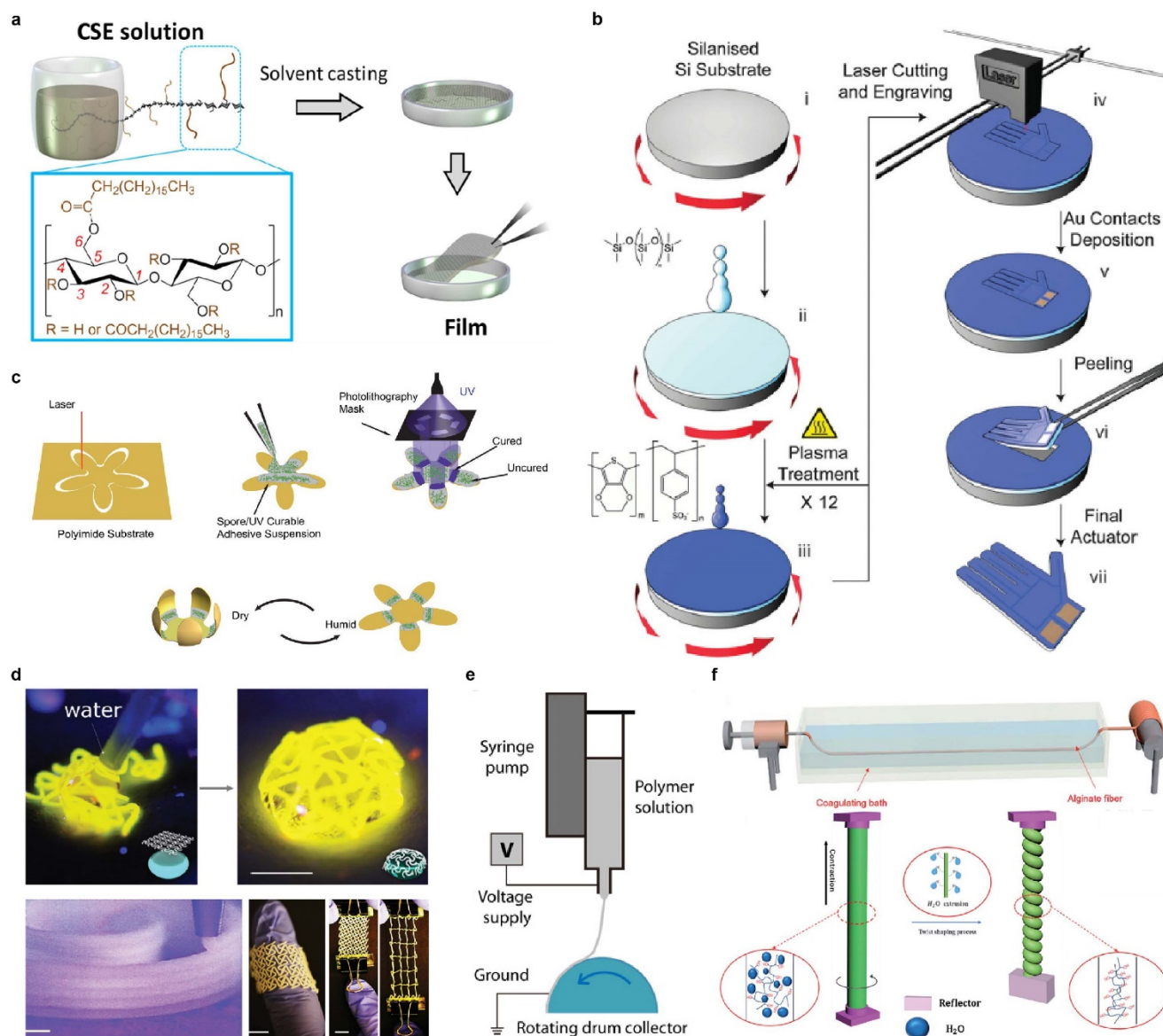


**Figure 7.** Examples of fabrication methods to prepare synthetic WR structures. (a) Fabrication of cellulose stearyl esters (CSE) films by solvent-casting method where CSE solution was poured onto substrate and dried to form films.<sup>94</sup> (b) Spin coated PEDOT:PSS films on a silicon wafer were laser cut into predetermined shapes.<sup>67</sup> (c) Fabrication of a WR “flower” with patterned spore/adhesive composites using photolithography.<sup>143</sup> (d) 3D printing of silicon beads/polydimethylsiloxane WR structures with complicated geometries.<sup>144</sup> (e) Electrospinning set up consisting of a syringe pump, a high voltage supply, and a collector prepares nanofibers of polymer solution.<sup>28</sup> (f) Wet spinning of alginate solution into a coagulating bath forms solidified WR fibres. Further twisting process amplifies WR actuation of the wet spun alginate fibre.<sup>145</sup> Reproduced from Ref <sup>94, 67, 143, 144, 28, 145</sup> with permission from Nature Publishing Group, John Wiley & Sons, Inc., The American Association for the Advancement of Science, The Royal Society of Chemistry.

Other methods, including photolithography,<sup>143, 149</sup> 3D printing,<sup>16, 150</sup> and fibre spinning,<sup>28, 124, 145, 151</sup> were also used to fabricate WR structures and program their motions. **Figure 7c** shows a representative example of using photolithographic method to make a pre-designed motion of a WR “flower” that consists of an active layer of spore/UV-curable adhesive composites. After mixing spores into UV-curable adhesive and depositing them on a passive polyimide substrate, UV light exposure cures spores/adhesive composites into patterns, which subsequently drive the blooming motions of the artificial flower in response to RH changes.<sup>143</sup> A similar photolithographic method was used in developing WR LC polymers, where the orientation of its internal mesogens was determined by UV curing.<sup>113, 114, 152</sup>

Recent development of 3D printing with the ability to fabricate structures with complex topography from nanoscale to macroscale and to extrude various types of materials from plastics to metals offers rapid prototyping and programming of WR motions. By integrating WR components into printable polymers, several 3D printed WR architectures have demonstrated complicated and programmable WR actuation (**Figure 7d**).<sup>16, 144, 150, 153</sup> Fibre spinning is another method that has been not only used by animals, but also widely used in industry to produce fibres with precisely controlled morphology from a wide range of polymer solutions. Electrospinning is one of the spinning methods that are often used to prepare fibres at nanoscales. By using the electrospinning whose setup simply

consists of a high voltage source, a syringe pump, and a collector, researchers deposited aligned hygroscopic PEO nanofibers in different directions on passive substrates to achieve various motions (Figure 7e).<sup>28, 109</sup> In addition to electrospinning, wet spinning process is a more industry-relevant technique to manufacture fibres. The wet spinning method was applied to fabricate WR alginate fibres by extruding sodium alginate solution through a syringe needle and solidifying the solution in a calcium chloride coagulation bath (Figure 7f).<sup>145</sup> The wet spun alginate fibre's diameter was well-controlled by the spinneret aperture and collecting speed of the rolling collector. Subsequently, the alginate fibres were twisted to amplify its WR actuation.<sup>145</sup> Similarly, WR GO fibres were also produced by direct wet spinning of GO suspension (20 mg ml<sup>-1</sup>) into methanol solution with 3 M KCl through a single-capillary spinneret.<sup>124</sup>

Understanding and further improving the performance of newly developed WR materials as actuators and energy conversion components are critical for their potential energy-related applications. However, commercially available equipment has a limited capability for characterizing materials' WR properties. By taking advantage of existing techniques used to characterize actuators and muscles, researchers have developed various methods to measure materials' WR properties.<sup>1, 8, 9, 32, 47, 58, 143</sup> These properties involve WR materials' characteristics under equilibrium (steady-state) conditions, including WR strain (%), stress (MPa), energy density (kJ m<sup>-3</sup>), and efficiency (%); and non-equilibrium (dynamic) conditions, including response time (s), specific power (W kg<sup>-1</sup>) or power density (W m<sup>-3</sup>), and cycle life.<sup>1, 8, 9, 32, 47, 58, 143</sup> To promote fundamental study of materials' WR behaviours and inspire development of new characterization methods and equipment, we briefly discuss currently available approaches to study WR materials' both steady-state and dynamic properties.

### 3. Water-Responsiveness Characterization

#### Methods

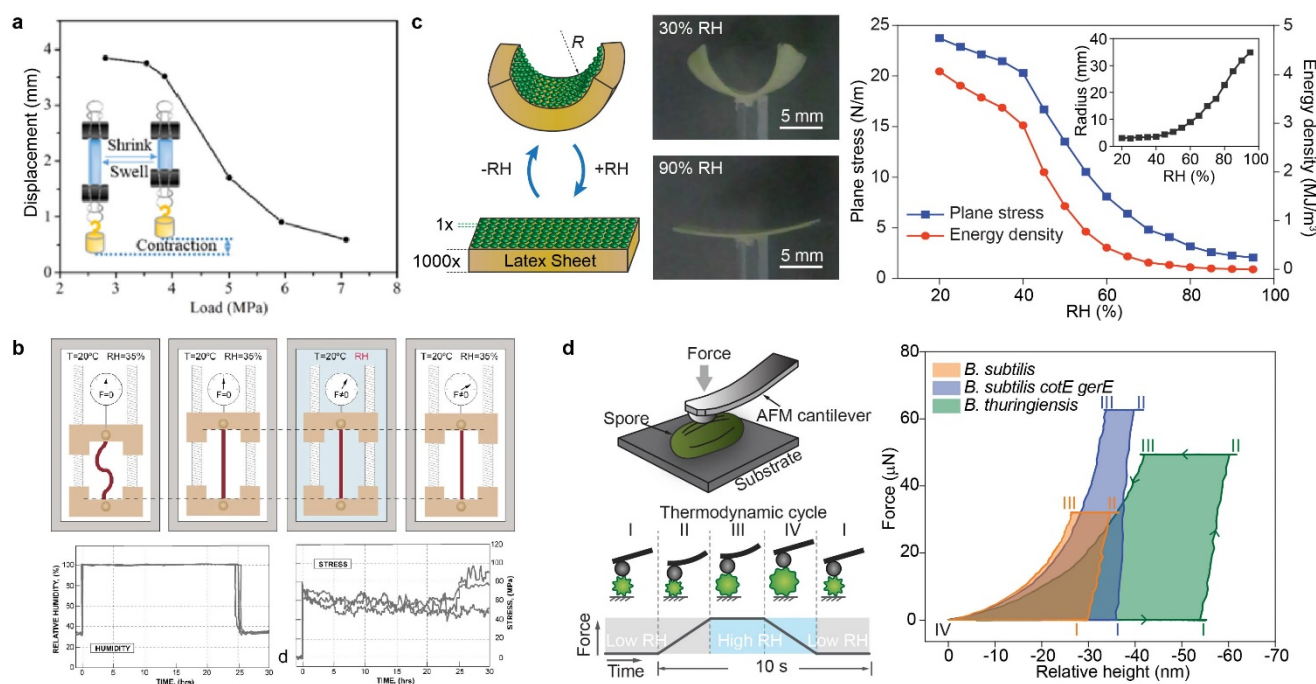


**Figure 8.** (a) The WR strain and stress of poly(3,4-ethylenedioxythiophene)/polyvinyl alcohol/copolymer of acrylic acid and 2-acrylamido-2-methylpropanesulfonic acid was measured under dry and wet conditions with different loads.<sup>154</sup> (b) WR stress of spider silk was measured by using a tensile testing machine with a humidity-controlled chamber. WR stress to maintain the strain of spider silk was recorded under high RH condition.<sup>47</sup> (c) Measured radius of curvature (inset) was used to estimate the plane stresses at the spore/rubber interface and WR energy density of the spore layer.<sup>1</sup> (d) Illustration of a thermodynamic cycle created by controlling the force and RH using an AFM.<sup>1</sup> Reproduced from ref.<sup>154, 47, 1</sup> with permission from American Chemical Society, Elsevier and Nature Publishing Group.

#### 3.1. Steady-state WR Behaviours

WR actuation relies on pressure changes induced by chemical potential difference of water inside the material and its vapour phase outside. When RH changes, the system's thermodynamic equilibrium changes from one state to another, leading to materials' WR actuation. WR actuation stops when the whole system re-reaches its equilibrium state. The steady-state WR

properties characterize WR properties under equilibrium conditions.

**Strain and stress** are general parameters to evaluate an actuator's or muscle's displacement normalized by its original length in the direction of actuation and the actuation force normalized by its cross-sectional area, respectively. WR strain is usually measured when the material of interest is exposed to two extreme RH conditions (~10% and ~90% RH). By varying

external loads applied during the strain test, WR stress can also be measured. For example, WR strain and stress of a poly(3,4-ethylenedioxythiophene)/polyvinyl alcohol/copolymer of acrylic acid and 2-acrylamido-2-methylpropanesulfonic acid film was measured under dry and wet conditions with different loads (**Figure 8a**).<sup>154</sup> The maximum WR stress that stops the material's WR actuation is called as blocking stress. To measure WR strain and stress, traditional tensile testing machines could be modified to be environmental-controlled. **Figure 8b** shows an example of how WR strain and stress of spider silk were measured using a tensile testing machine within a chamber where the RH was precisely controlled.<sup>47</sup> Most of these WR strain/stress testing methods require standing alone samples with a minimum size of millimetre scales. However, many of newly developed WR materials are either fabricated into bilayer structures or too small to be tested by traditional tensile testing methods. For WR bilayer structures, WR stress can be estimated by monitoring their curvature changes at different RHs. As shown in **Figure 8c**, the plane stress of WR active layer at 10% RH can be estimated by equation (1):<sup>1, 58, 143</sup>

$$\sigma_x = \frac{Et^2}{\sigma(1-\nu^2)} \left( \frac{1}{R_x} - \nu \frac{1}{R_y} \right) \quad (1)$$

where  $\sigma_x$  is the surface stress along the direction of the observed curvature,  $E$  is Young's modulus of the passive substrate,  $\nu$  is Poisson's coefficient for the passive substrate,  $t$  is the thickness of the passive substrate and  $R_x, R_y$  are the radii of the curvature. For WR materials at nanoscale, we have developed an environmental-controlled AFM where local RH can be varied while monitoring the height change and actuation force of WR materials. By using this method, we have measured the WR strain of various nanoscale spores in response to alternating RH between  $\sim 15\%$  to  $\sim 90\%$ .<sup>1</sup>

**Energy density**, also known as work density, measures the amount of work done by a WR actuator in one hydration and dehydration cycle normalized by its unit volume. For the bilayer structure shown in **Figure 8c**, since work done by the active layer is equivalent to elastic energy stored in the curved active/passive bilayer structure, we can estimate WR materials' actuation energy ( $U$ ) by using equation (2):<sup>1, 58, 143</sup>

$$U = \frac{(E_1 I_1 + E_2 I_2)L}{R^2} \quad (2)$$

where  $E_1$  and  $E_2$  are the Young's modulus of the active layer and passive substrate, respectively.  $I_1$  and  $I_2$  are the area moment of inertia of the active layer and the passive substrate, respectively. Energy density can be subsequently calculated by dividing WR materials' volume in the active layer.

In addition, we customized an AFM setup to measure the maximum work done by nanoscale WR materials within single hydration and dehydration cycle and developed a computer program to create the thermodynamic cycle where WR materials are subjected to periodically varying forces and RH. The thermodynamic cycle with changing forces and RH

levels is composed of four stages as illustrated in **Figure 8d**.<sup>1</sup> In stage I, the spores rest at low RH. The AFM probe is put in contact with the spores using a negligibly small force—just enough to maintain contact. In stage II, the cantilever exerts a predetermined force (loading). The spores respond by reducing their overall height. In stage III, the spores are subjected to high RH while the force is maintained constant. Spores respond to increasing RH by expanding and pushing the cantilever away from the surface. In stage IV, the force is reduced back to zero. The cycle is completed by lowering the RH to the initial level. Energy density can be determined by dividing the work done in one thermodynamic cycle to the volume contributing to the WR work.<sup>1</sup>

**Efficiency or energy conversion efficiency** is the ratio of materials' WR actuation energy output to its energy input. Usually, energy input is the chemical potential differences of absorbed/desorbed water molecules and energy output is the mechanical work generated by the WR.<sup>77</sup> Therefore, energy conversion efficiency of the WR material can be estimated from its energy density, the amount of absorbed/desorbed water, and water's chemical potential differences.<sup>77</sup> Many existing techniques can accurately measure materials' water exchange, including dynamic vapour sorption (DVS) which was used to measure the WR silk's mass changes at predefined RH cycles.<sup>58</sup>

### 3.2. Dynamic WR Behaviours

Materials' WR dynamic behaviours describe their water-responsiveness when they are out of equilibrium conditions. **Response time** (or speed) of a WR material shows how fast the material re-reaches the equilibrium during WR actuation. Response time ( $\tau$ ) of a bilayer WR material can be calculated by fitting WR bending to an exponential curve  $1/r = a + be^{-\frac{t}{\tau}}$  using the least squares method where  $r$  is the radius of the curvature,  $a$  and  $b$  are regression coefficients, and  $t$  is the time. **Figure 9a** shows that, by fitting a spore/polyimide bilayer structure's curvature changes over time to the exponential curve, the response time was estimated as 4.2–14.8 s when the bilayer structure experiencing alternating RHs between 10 % and 90 %. **Power density** (specific power) that describes how fast a WR actuator can release a certain amount of energy can be estimated by dividing its energy density by its response time (**Figure 9b**). **Cycle life** (or lifetime) is the number of actuation that the WR material can perform until any major attenuation of its performance or failures of its structures. **Figure 9c** shows a negligible reduction in WR displacement of spore/polyimide bilayer structures after 1 million hydration and dehydration cycles.<sup>1</sup> Another study of degummed silkworm silk fibres that were twisted to form torsional silk muscles demonstrated a reversible torsional stroke upon exposure to ultrasonically generated fog for multiple cycles in an open circulating environment (20%RH, 25 °C) (**Figure 9d-e**).<sup>26</sup>

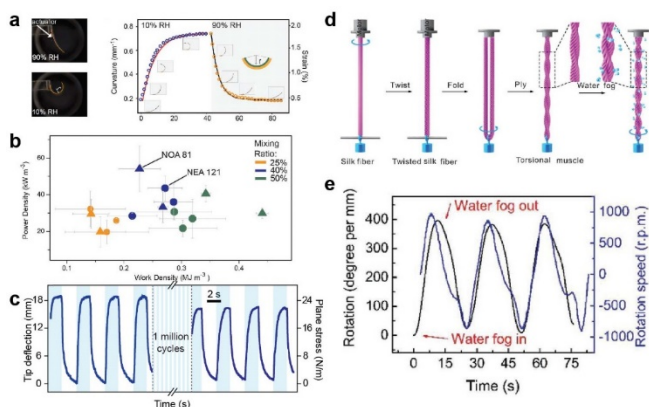


**Figure 9.** (a-b) The response time of a WR spore/UV-curable adhesive was measured from changes in its curvature ( $1/r$ ) over time. Its power density was subsequently calculated by dividing the energy density by the response time.<sup>143</sup> (c) Displacement of a WR coated AFM cantilever reduced slightly after one million cycles of alternating RH.<sup>1</sup> (d-e) Twisted degummed silkworm silk fibres reversibly rotate upon changes in RH.<sup>26</sup> Reproduced from ref <sup>1, 143, 26</sup> with permission from John Wiley & Sons, Inc., Nature Publishing Group, and The Royal Society of Chemistry.

#### 4. Perspectives for Future Research

WR materials that powerfully deform during hydration and dehydration cycles have enabled various energy-related applications, including ambient RH fluctuation and natural evaporation energy harvesting,<sup>1, 9, 10, 15</sup> artificial muscles,<sup>119</sup> smart textiles,<sup>27</sup> and smart building materials.<sup>18, 19</sup> However, the use of WR materials in energy-related applications is mainly restricted by the limited knowledge about how to design high-efficiency WR actuators. Despite a great number of demonstrations, it remains difficult to understand the fundamental mechanisms of materials' water-responsiveness and energy transfer processes, especially at molecular level. Many high-performance WR materials contain hierarchical and nanoporous structures such as bacterial spores,<sup>1</sup> CNT hybrid yarns,<sup>119</sup> and engineered protein films.<sup>118</sup> It is very likely that, water molecules at solid-liquid interfaces in these nanopores exhibit very different physical and chemical properties compared to bulk water, which could play a crucial role in their overall energy conversion processes. Thus, to fully understand WR mechanisms, it is essential to understand water's behaviour at the nano- and sub-micro scale, including chemical potential difference induced pressure and structural changes. Further studies on nanoconfined water within WR materials using both experimental and computational approaches could help reveal the mystery behind materials' powerful WR behaviours.

The device design is another challenge to demonstrate the feasibility of using WR materials for practical applications. Since there is very limited commercially available engineering system that can be used to work with this new kind of WR actuators, researchers are often required to develop their own devices. For example, we have designed oscillatory and rotary engines with mechanical feedback systems to demonstrate the potential of using WR bacterial spores to directly and continuously harvest energy from natural evaporation.<sup>1,9</sup> However, a proper mechanical design usually requires a great

amount of interdisciplinary work, which could be challenge for individual research groups. We envision that increasing collaborative efforts between scientists and engineers could dramatically speedup the development of various devices that could be used to demonstrate WR materials' potential, and even to be commercialized.

In addition, current limitations of commercially available equipment for characterizing and fabricating WR materials also restrict their development. As discussed, some researchers have modified existing analytical techniques to test materials' WR properties, including WR strain, stress, efficiency, responsive speed, energy density and power density, which are of great importance for energy-related applications. For examples, a tensile testing machine and an AFM that were customized to be RH-controlled can measure WR strain and stress of materials at millimetre-scale and nanoscale, respectively.<sup>1, 8, 47</sup> These studies provide great examples to standardize characterization methods specifically for materials' water-responsiveness and promote future development of commercial testing equipment. Despite excellent examples of natural and synthetic WR materials we discussed, in particular, bacterial spores,<sup>1</sup> natural and regenerated silk,<sup>8, 58</sup> and CNT based composites,<sup>119</sup> efficiently scaling up materials' water-responsiveness is also critical for practical applications. Many of current proof-of-concept demonstrations are based on millimetre-scale or centimetre-scale WR materials of film and fibre structures.<sup>10, 15, 29, 58, 119, 124, 145</sup> Further studies on fabrication of WR structures by utilizing existing industrial manufacturing techniques seem promising. For instance, 3D printing that manufactures complicated geometries could be a great avenue to program and scale up materials' water-responsiveness. We hope our review on current progresses of WR materials could inspire future studies to establish general rules for design and fabrication of high-efficiency WR materials.

#### Acknowledgements

This work was supported by The Office of Naval Research (ONR) (N00014-18-1-2492). We appreciate Raymond S. Tu and Qixing (Jacky) Zhang for helpful comments on our manuscript.

#### References

- Chen, X.; Mahadevan, L.; Driks, A.; Sahin, O., Bacillus spores as building blocks for stimuli-responsive materials and nanogenerators. *Nature Nanotechnology* **2014**, *9*, 137-141.
- Pelrine, R.; Kornbluh, R.; Pei, Q. B.; Joseph, J., High-speed electrically actuated elastomers with strain greater than 100%. *Science* **2000**, *287* (5454), 836-839.
- Haines, C. S.; Lima, M. D.; Li, N.; Spinks, G. M.; Foughi, J.; Madden, J. D. W.; Kim, S. H.; Fang, S. L.; de Andrade, M. J.; Goktepe, F.; Goktepe, O.; Mirvakili, S. M.; Naficy, S.; Lepro, X.; Oh, J. Y.; Kozlov, M. E.; Kim, S. J.; Xu, X. R.; Swedlove, B. J.; Wallace, G. G.; Baughman, R. H., Artificial Muscles from Fishing Line and Sewing Thread. *Science* **2014**, *343* (6173), 868-872.
- Jiang, H. Y.; Kelch, S.; Lendlein, A., Polymers move in response to light. *Adv Mater* **2006**, *18* (11), 1471-1475.

5. Thevenot, J.; Oliveira, H.; Sandre, O.; Lecommandoux, S., Magnetic responsive polymer composite materials. *Chem Soc Rev* **2013**, *42* (17), 7099-7116.
6. He, X. M.; Aizenberg, M.; Kuksenok, O.; Zarzar, L. D.; Shastri, A.; Balazs, A. C.; Aizenberg, J., Synthetic homeostatic materials with chemo-mechano-chemical self-regulation. *Nature* **2012**, *487* (7406), 214-218.
7. Mary Elaine Gage, J. E. G., *The Art of Splitting Stone: Early Rock Quarrying Methods in Pre-industrial New England, 1630-1825*. Powwow River Books: 2005.
8. Agnarsson, I.; Dhinojwala, A.; Sahni, V.; Blackledge, T. A., Spider silk as a novel high performance biomimetic muscle driven by humidity. *The Journal of Experimental Biology* **2009**, *212*, 1990-1994.
9. Chen, X.; Goodnight, D.; Gao, Z.; Cavusoglu, A. H.; Sabharwal, N.; DeLay, M.; Driks, A.; Sahin, O., Scaling up nanoscale water-driven energy conversion into evaporation-driven engines and generators. *Nature Communications* **2015**, *6*.
10. Ma, M.; Guo, L.; Anderson, D. G.; Langer, R., Bio-Inspired Polymer Composite Actuator and Generator Driven by Water Gradients. *Science* **2013**, *339*, 186-189.
11. Dawson, C.; Vincent, J. F. V.; Rocca, A.-M., How pine cones open. *Nature* **1997**, *390*, 668.
12. Elbaum, R.; Zaltzman, L.; Burgert, I.; Fratzl, P., The Role of Wheat Awns in the Seed Dispersal Unit. *Science* **2007**, *316*, 884-886.
13. Harrington, M. J.; Razghandi, K.; Ditsch, Friedrich; Guiducci, L.; Rueggeberg, M.; Dunlop, J. W. C.; Fratzl, P.; Neinhuis, C.; Burgert, I., Origami-like unfolding of hydro-actuated ice plant seed capsules. *Nature Communications* **2011**, *2*, 337.
14. Liu, D.; Tarakanova, A.; Hsu, C. C.; Yu, M.; Zheng, S.; Yu, L.; Liu, J.; He, Y.; Dunstan, D. J.; Buehler, M. J., Spider dragline silk as torsional actuator driven by humidity. *Science Advances* **2019**, *5*, eaau9183.
15. Arazoe, H.; Miyajima, D.; Akaike, K.; Araoka, F.; Sato, E.; Hikima, T.; Kawamoto, M.; Aida, T., An autonomous actuator driven by fluctuations in ambient humidity. *Nature Materials* **2016**, *15*, 1084-1090.
16. Gladman, A. S.; Matsumoto, E. A.; Nuzzo, R. G.; Mahadevan, L.; Lewis, J. A., Biomimetic 4D printing. *Nature Materials* **2016**, *15*, 413-418.
17. Mu, J.; Andrade, M. J. d.; Fang, S.; Wang, X.; Gao, E.; Li, N.; Kim, S. H.; Wang, H.; Hou, C.; Zhang, Q.; Zhu, M.; Qian, D.; Lu, H.; Kongahage, D.; Talebian, S.; Foroughi, J.; Spinks, G.; Kim, H.; Ware, T. H.; Sim, H. J.; Lee, D. Y.; Jang, Y.; Kim, S. J.; Baughman, R. H., Sheath-run artificial muscles. *Science* **2019**, *365*, 150-155.
18. Holstov, A.; Bridgens, B.; Farmer, G., Hygromorphic materials for sustainable responsive architecture. *Construction and Building Materials* **2015**, *98*, 570-582.
19. Menges, A.; Reichert, S., Material Capacity: Embedded Responsiveness. *Architectural Design* **2012**, *82*, 52-59.
20. Lv, C.; Sun, X.-C.; Xu, Y.-S.; Zhang, W.-Y.; Li, P.; Shi, Q.; Wang, L.; Wang, G.; Cao, X.-W.; Li, S.-X.; Dai, Y.-Z.; Xia, H., Actuation From Directional Deformation Based on Composite Hydrogel for Moisture-Controllable Devices. *IEEE SENSORS JOURNAL* **2018**, *18*, 8796-8802.
21. Islam, M. R.; Li, X.; Smyth, K.; Serpe, M. J., Polymer-Based Muscle Expansion and Contraction. *Angewandte Chemie International Edition* **2013**, *52*, 10330-10333.
22. He, S.; Chen, P.; Qiu, L.; Wang, B.; Sun, X.; Xu, Y.; Peng, H., A Mechanically Actuating Carbon-Nanotube Fiber in Response to Water and Moisture. *Angewandte Chemie International Edition* **2015**, *54*, 14880-14884.
23. Mu, J.; Hou, C.; Zhu, B.; Wang, H.; Li, Y.; Zhang, Q., A multi-responsive water-driven actuator with instant and powerful performance for versatile applications. *Scientific Report* **2015**, *5*.
24. Gong, J.; Lin, H.; Dunlop, J. W. C.; Yuan, J., Hierarchically Arranged Helical Fiber Actuators Derived from Commercial Cloth. *Adv Mater* **2017**, *29*.
25. Mu, J.; Wang, G.; Yan, H.; Li, H.; Wang, X.; Gao, E.; Hou, C.; Pham, A. T. C.; Wu, L.; Zhang, Q.; Li, Y.; Xu, Z.; Guo, Y.; Reichmanis, E.; Wang, H.; Zhu, M., Molecular-channel driven actuator with considerations for multiple configurations and color switching. *Nature Communications* **2018**, *9*.
26. Jia, T.; Wang, Y.; Dou, Y.; Li, Y.; Andrade, M. J. d.; Wang, R.; Fang, S.; Li, J.; Yu, Z.; Qiao, R.; Liu, Z.; Cheng, Y.; Su, Y.; Minary-Jolandan, M.; Baughman, R. H.; Qian, D.; Liu, Z., Moisture Sensitive Smart Yarns and Textiles from Self-Balanced Silk Fiber Muscles. *Advanced Functional Materials* **2019**, *29*, 1808241.
27. Wang, W.; Yao, L.; Cheng, C.-Y.; Zhang, T.; Atsumi, H.; Wang, L.; Wang, G.; Anilionyte, O.; Steiner, H.; Ou, J.; Zhou, K.; Wawrousek, C.; Petrecca, K.; Belcher, A. M.; Karnik, R.; Zhao, X.; Wang, D. I. C.; Ishii, H., Harnessing the hygroscopic and biofluorescent behaviors of genetically tractable microbial cells to design biohybrid wearables. *SCIENCE ADVANCES* **2017**, *3*, e160198.
28. Shin, B.; Ha, J.; Lee, M.; Park, K.; Park, G. H.; Choi, T. H.; Cho, K.-J.; Kim, H.-Y., Hygrobot: A self-locomotive ratcheted actuator powered by environmental humidity. *Science Robotics* **2018**, *3*.
29. Cheng, H.; Liu, J.; Zhao, Y.; Hu, C.; Zhang, Z.; Chen, N.; Jiang, L.; Qu, L., Graphene Fibers with Predetermined Deformation as Moisture-Triggered Actuators and Robots. *Angewandte Chemie International Edition* **2013**, *52*, 10482-10486.
30. Ryu, J.; Mohammadifar, M.; Tahernia, M.; Chun, H.-i.; Gao, Y.; Choi, S., Paper Robotics: Self-Folding, Gripping, and Locomotion. *Advanced Materials Technologies* **2020**, 1901054.
31. Cavusoglu, A.-H.; Chen, X.; Gentine, P.; Sahin, O., Potential for natural evaporation as a reliable renewable energy resource. *Nature Communications* **2017**, *8*.
32. Madden, J. D. W.; Vandesteeg, N. A.; Anquetil, P. A.; Madden, P. G. A.; Takshi, A.; Pytel, R. Z.; Lafontaine, S. R.; Wieringa, P. A.; Hunter, I. W., Artificial Muscle Technology: Physical Principles and Naval Prospects. *IEEE Journal of Oceanic Engineering* **2004**, *29*, 706-728.
33. Zhao, Q.; Wang, Y.; Cui, H.; Du, X., Bio-inspired sensing and actuating materials. *Journal of Materials Chemistry C* **2019**, *7*, 6493-6511.
34. Hines, L.; Petersen, K.; Lum, G. Z.; Sitti, M., Soft Actuators for Small-Scale Robotics. *Adv Mater* **2017**, *29*, 1603483.
35. Evangelista, D.; Hotton, S.; Dumais, J., The mechanics of explosive dispersal and self-burial in the seeds of the filaree, *Erodium cicutarium* (Geraniaceae). *The Journal of Experimental Biology* **2011**, *214*, 521-529.
36. Ha, J.; Choi, S. M.; Shin, B.; Lee, M.; Jung, W.; Kim, H.-Y., Hygroresponsive coiling of seed awns and soft actuators. *Extreme Mechanics Letters* **2020**, *38*, 100746.
37. Elbaum, R.; Gorb, S.; Fratzl, P., Structures in the cell wall that enable hygroscopic movement of wheat awns. *Journal of Structural Biology* **2008**, *164*, 101-110.
38. Reyssat, E.; Mahadevan, L., Hygromorphs: from pine cones to biomimetic bilayers. *Journal of the Royal Society Interfaces* **2009**, *6*, 951-957.
39. Yanez, A.; Desta, I.; Commins, P.; Magzoub, M.; Naumov, P. e., Morphokinematics of the Hygroactuation of Feather Grass Awns. *Advanced Biosystems* **2018**, *2*, 1800007.

40. Song, K.; Yeom, E.; Seo, S.-J.; Kim, K.; Kim, H.; Lim, J.-H.; Lee, S. J., Journey of water in pine cones. *Scientific Report* **2015**, *5*, 09963.
41. Meng, Q. a.; Wang, Q.; Zhao, K.; Wang, P.; Liu, P.; Liu, H.; Jiang, L., Hydroactuated Configuration Alteration of Fibrous Dandelion Pappi: Toward Self-Controllable Transport Behavior. *Advanced Functional Materials* **2016**, *26*, 7378-7385.
42. Abraham, Y.; Elbaum, R., Hygroscopic movements in Geraniaceae: the structural variations that are responsible for coiling or bending. *New Phytologist* **2013**, *199*, 584-594.
43. Abraham, Y.; Tamburu, C.; Klein, E.; Dunlop, J. W. C.; Fratzl, P.; Raviv, U.; Elbaum, R., Tilted cellulose arrangement as a novel mechanism for hygroscopic coiling in the stork's bill awn. *Journal of the Royal Society Interfaces* **2012**, *9*, 640-647.
44. Erb, R. M.; Sander, J. S.; Grisch, R.; Studart, A. R., Self-shaping composites with programmable bioinspired microstructures. *Nature Communications* **2013**, *4*, 1712.
45. Boutry, C.; Blackledge, T. A., Evolution of supercontraction in spider silk: structure–function relationship from tarantulas to orb-weavers. *The Journal of Experimental Biology* **2010**, *213*, 3505-3514.
46. Agnarsson, I.; Boutry, C.; Wong, S.-C.; Baji, A.; Dhinojwala, A.; Sensenig, A. T.; Blackledge, T. A., Supercontraction forces in spider dragline silk depend on hydration rate. *Zoology* **2009**, *112*, 325-331.
47. Guinea, G. V.; Elices, M.; Perez-Rigueiro, J.; Plaza, G., Self-tightening of spider silk fibers induced by moisture. *Polymer* **2003**, *44*, 5785-5788.
48. Bowen, C. H.; Dai, B.; Sargent, C. J.; Bai, W. Q.; Ladiwala, P.; Feng, H. B.; Huang, W. W.; Kaplan, D. L.; Galazka, J. M.; Zhang, F. Z., Recombinant Spidroins Fully Replicate Primary Mechanical Properties of Natural Spider Silk. *Biomacromolecules* **2018**, *19* (9), 3853-3860.
49. Fink, T. D.; Zha, R. H., Silk and Silk-Like Supramolecular Materials. *Macromolecular Rapid Communications* **2018**, *39*.
50. Xiao, X.; Hu, J., Animal Hairs as Water-stimulated Shape Memory Materials: Mechanism and Structural Networks in Molecular Assemblies. *Scientific Report* **2016**, *6*, 26393.
51. Xiao, X.; Hu, J.; Gui, X.; Lu, J.; Luo, H., Is biopolymer hair a multi-responsive smart material? *Polymer Chemistry* **2017**, *8*, 283-294.
52. Blackledge, T. A.; Boutry, C.; Wong, S.-C.; Baji, A.; Dhinojwala, A.; Sahni, V., How super is supercontraction? Persistent versus cyclic responses to humidity in spider dragline silk. *The Journal of Experimental Biology* **2009**, *212*, 1981-1989.
53. Liu, Y.; Shao, Z.; Vollarth, F., Relationships between supercontraction and mechanical properties of spider silk. *Nature Materials* **2005**, *4*, 901-905.
54. Westphal, A. J.; Price, P. B.; Leighton, T. J.; Wheeler, K. E., Kinetics of size changes of individual *Bacillus thuringiensis* spores in response to changes in relative humidity. *PNAS* **2003**, *100*, 3461-3466.
55. Driks, A., The dynamic spore. *PNAS* **2003**, *100*, 3007-3009.
56. Reyssat, E.; Mahadevan, L., How wet paper curls. *Europhysics Letters* **2011**, *93*.
57. Zhao, Z.; Hwang, Y.; Yang, Y.; Fan, T.; Song, J.; Suresh, S.; Cho, N.-J., Actuation and locomotion driven by moisture in paper made with natural pollen. *PNAS* **2020**.
58. Park, Y.; Jung, Y.; Li, T.-D.; Lao, J.; Tu, R.; Chen, X.,  $\beta$ -sheet nanocrystals dictate water-responsiveness of *Bombyx mori* silk. *Macromolecular Rapid Communications* **2020**, *41*, 1900612.
59. Gao, F.; Zhang, N.; Fang, X.; Ma, M., Magnetically directed soft actuators driven by moisture. *Journal of Materials Chemistry C* **2017**, *5*, 4219-4133.
60. Wang, T.; Li, M.; Zhang, H.; Sun, Y.; Dong, B., A multi-responsive bidirectional bending actuator based on polypyrrole and agar nanocomposites. *Journal of Materials Chemistry C* **2018**, *6*, 6416-6422.
61. Kuang, Y.; Chen, C.; Cheng, J.; Pastel, G.; Li, T.; Song, J.; Jiang, F.; Li, Y.; Zhang, Y.; Jang, S.-H.; Chen, G.; Li, T.; Hu, L., Selectively aligned cellulose nanofibers towards high-performance soft actuators. *Extreme Mechanics Letters* **2019**, *29*.
62. Zong, L.; Li, M.; Li, C., Bioinspired Coupling of Inorganic Layered Nanomaterials with Marine Polysaccharides for Efficient Aqueous Exfoliation and Smart Actuating Hybrids. *Adv Mater* **2017**, *29*.
63. Cai, G.; Ciou, J.-H.; Liu, Y.; Jiang, Y.; Lee, P. S., Leaf-inspired multiresponsive MXene-based actuator for programmable smart devices. *Science Advances* **2019**, *5*.
64. Ma, Y.; Zhang, Y.; Wu, B.; Sun, W.; Li, Z.; Sun, J., Polyelectrolyte Multilayer Films for Building Energetic Walking Devices. *Angewandte Chemie International Edition* **2011**, *50*, 6254-6257.
65. Chen, L.; Weng, M.; Huang, F.; Zhang, W., Light- and humidity-driven actuators with programmable complex shape-deformations. *Sensors and Actuators B: Chemical* **2019**, *282*, 384-390.
66. Li, B.; Du, T.; Yu, B.; Gucht, J. v. d.; Zhou, F., Caterpillar-Inspired Design and Fabrication of A Self-Walking Actuator with Anisotropy, Gradient, and Instant Response. *Small* **2015**, *11*, 3494-3501.
67. Taccola, S.; Greco, F.; Sinibaldi, E.; Mondini, A.; Mazzolai, B.; Mattoli, V., Toward a New Generation of Electrically Controllable Hygromorphic Soft Actuators. *Adv Mater* **2015**, *27*, 1668-1675.
68. Xu, H.; Xu, X.; Xu, J.; Dai, S.; Dong, X.; Han, F.; Yuan, N.; Ding, J., An ultra-large deformation bidirectional actuator based on a carbon nanotube/PDMS composite and a chitosan film. *Journal of Materials Chemistry B* **2019**, *7*, 7558-7565.
69. Qiu, Y.; Wang, M.; Zhang, W.; Liu, Y.; Li, Y. V.; Pan, K., An asymmetric graphene oxide film for developing moisture actuators. *Nanoscale* **2018**, *10*, 14060-14066.
70. Ji, X.; Ying, Y.; Ge, C.; Zhu, Y.; Wang, K.; Di, Y.; Wang, S.; Li, D.; zhang, J.; Hu, P.; Qiu, Y., Asymmetrically synchronous reduction and assembly of graphene oxide film on metal foil for moisture responsive actuator. *Nanotechnology* **2019**, *30*.
71. Zhong, Y.; Zhang, F.; Wang, M.; Gardner, C. J.; Kim, G.; Liu, Y.; Leng, J.; Jin, S.; Chen, R., Reversible Humidity Sensitive Clothing for Personal Thermoregulation. *Scientific Report* **2017**, *7*.
72. Chen, M.; Frueh, J.; Wang, D.; Lin, X.; Xie, H.; He, Q., Polybenzoxazole Nanofiber-Reinforced Moisture-Responsive Soft Actuators. *Scientific Report* **2017**, *7*.
73. Weng, M.; Zhou, P.; Chen, L.; Zhang, L.; Zhang, W.; Huang, Z.; Liu, C.; Fan, S., Multiresponsive Bidirectional Bending Actuators Fabricated by a Pencil-on-Paper Method. *Advanced Functional Materials* **2016**, *26*, 7244-7253.
74. Zhang, L.; Naumov, P. e., Light- and Humidity-Induced Motion of an Acidochromic Film. *Angewandte Chemie International Edition* **2015**, *54*, 8642-8647.
75. Zhang, L.; Liang, H.; Jacob, J.; Naumov, P. e., Photogated humidity-driven motility. *Nature Communications* **2015**, *6*.
76. Zhang, L.; Chizhik, S.; Wen, Y.; Naumov, P. e., Directed Motility of Hygroresponsive Biomimetic Actuators. *Advanced Functional Materials* **2016**, *26*, 1040-1053.
77. Tan, H.; Yu, X.; Tu, Y.; Zhang, L., Humidity-Driven Soft Actuator Built up Layer-by-Layer and Theoretical Insight into Its Mechanism of Energy Conversion. *The Journal of Physical Chemistry Letters* **2019**, *10*, 5542-5551.
78. Ren, Z.; Ding, Y.; Nie, J.; Wang, F.; Xu, L.; Lin, S.; Chen, X.; Wang, Z. L., Environmental Energy Harvesting Adapting to Different Weather Conditions and Self-Powered Vapor Sensor Based on Humidity-Responsive Triboelectric Nanogenerators. *ACS Applied Materials & Interfaces* **2019**, *11*, 6143-3153.

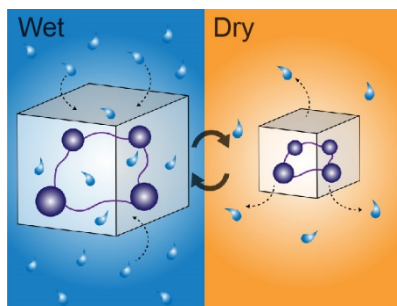
79. Castaldo, R.; Lama, G. C.; Aprea, P.; Gentile, G.; Ambrogi, V.; Lavorgna, M.; Cerruti, P., Humidity-Driven Mechanical and Electrical Response of Graphene/Cloisite Hybrid Films. *Advanced Functional Materials* **2019**, *29*.
80. Palleau, E.; Morales, D.; Dickey, M. D.; Velev, O. D., Reversible patterning and actuation of hydrogels by electrically assisted ionoprinting. *Nature Communications* **2013**, *4*, 2257.
81. Wang, G.; Xia, H.; Sun, X.-C.; Lv, C.; Li, S.-X.; Han, B.; Guo, Q.; Shi, Q.; Wang, Y.-S.; Sun, H.-B., Actuator and generator based on moisture-responsive PEDOT:PSS/PVDF composite film. *Sensors and Actuators B: Chemical* **2018**, *255*, 1415-1421.
82. Zhou, J.; Wu, C.; Wu, D.; Wang, Q.; Chen, Y., Humidity-sensitive polymer xerogel actuators prepared by biaxial pre-stretching and drying. *Chemical Communications* **2018**, *54*, 11610-11613.
83. Lv, C.; Xia, H.; Shi, Q.; Wang, G.; Wang, Y.-S.; Chen, Q.-D.; Zhang, Y.-L.; Liu, L.-Q.; Sun, H.-B., Sensitive Humidity-Driven Actuator Based on Photopolymerizable PEG-DA Films. *Advanced Materials Interfaces* **2017**, *4*.
84. Salvekar, A. V.; Huang, W. M.; Xiao, R.; Wong, Y. S.; Venkatraman, S. S.; Tay, K. H.; Shen, Z. X., Water-Responsive Shape Recovery Induced Buckling in Biodegradable Photo-Cross-Linked Poly(ethylene glycol) (PEG) Hydrogel. *Accounts Chem Res* **2017**, *50* (2), 141-150.
85. Lv, C.; Sun, X.-C.; Xia, H.; Yu, Y.-H.; Wang, G.; Cao, X.-W.; Li, S.-X.; Wang, Y.-S.; Chen, Q.-D.; Yu, Y.-D.; Sun, H.-B., Humidity-responsive actuation of programmable hydrogel microstructures based on 3D printing. *Sensors and Actuators B: Chemical* **2018**, *259*, 736-744.
86. Wu, Y.; Shah, D. U.; Wang, B.; Liu, J.; Ren, X.; Ramage, M. H.; Scherman, O. A., Biomimetic Supramolecular Fibers Exhibit Water-Induced Supercontraction. *Adv Mater* **2018**, *30*.
87. Zhang, L.; Qiu, X.; Yuan, Y.; Zhang, T., Humidity- and Sunlight-Driven Motion of a Chemically Bonded Polymer Bilayer with Programmable Surface Patterns. *ACS Applied Materials & Interfaces* **2017**, *9*, 41599-41606.
88. Qiu, X.; Liang, S.; Huang, X.; Zhang, L., Pre-patterning and post-oxidation-crosslinking of Fe(0) particles for a humidity-sensing actuator. *Chemical Communications* **2019**, *55*, 15049-15052.
89. Morales, D.; Podolsky, I.; Mailen, R. W.; Shay, T.; Dickey, M. D.; Velev, O. D., Ionoprinted Multi-Responsive Hydrogel Actuators. *Micromachines* **2016**, *7*.
90. Chung, J. Y.; King, H.; Mahadevan, L., Evaporative microclimate driven hygrometers and hygromotors. *Europhysics Letters* **2014**, *107*.
91. Wang, M.; Tian, X.; Ras, R. H. A.; Ikkal, O., Sensitive Humidity-Driven Reversible and Bidirectional Bending of Nanocellulose Thin Films as Bio-Inspired Actuation. *Advanced Materials Interfaces* **2015**, *2*, 1500080.
92. Bettotti, P.; Maestri, C. A.; Guider, R.; Mancini, I.; Nativ-Roth, E.; Golan, Y.; Scarp, M., Dynamics of Hydration of Nanocellulose Films. *Advanced Materials Interfaces* **2016**, *2016*, 1500415.
93. Trembl, B. E.; McKenzie, R. N.; Buskohl, P.; Wang, D.; Kuhn, M.; Tan, L.-S.; Vaia, R. A., Autonomous Motility of Polymer Films. *Adv Mater* **2018**, *30*.
94. Zhang, K.; Geissler, A.; Standhardt, M.; Mehlhase, S.; Gallei, M.; Chen, L.; Thiele, C. M., Moisture-responsive films of cellulose stearoyl esters showing reversible shape transitions. *Scientific Report* **2015**, *5*.
95. Wang, D. H.; McKenzie, R. N.; Buskohl, P. R.; Vaia, R. A.; Tan, L.-S., Hygromorphic Polymers: Synthesis, Retro-Michael Reaction, and Humidity-Driven Actuation of Ester-Sulfonyl Polyimides and Thermally Derived Copolyimides. *Macromolecules* **2016**, *49*, 3286-3299.
96. Tseng, I.-H.; Li, J.-J.; Chang, P.-Y., Mimosa Pudica Leaf-Like Rapid Movement and Actuation of Organosoluble Polyimide Blending with Sulfonated Polyaniline. *Advanced Materials Interfaces* **2017**, *4*, 1600901.
97. Xie, Y.; Lei, D.; Wang, S.; Liu, Z.; Sun, L.; Zhang, J.; Qing, F.-L.; He, C.; You, Z., A Biocompatible, Biodegradable, and Functionalizable Copolyester and Its Application in Water-Responsive Shape Memory Scaffold. *ACS Biomaterials Science & Engineering* **2019**, *5*, 1668-1676.
98. Wong, Y. S.; Salvekar, A. V.; Zhuang, K. D.; Liu, H.; Birch, W. R.; Tay, K. H.; Huang, W. M.; Venkatraman, S. S., Bioabsorbable radiopaque water-responsive shape memory embolization plug for temporary vascular occlusion. *Biomaterials* **2016**, *102*, 98-106.
99. Yang, G.; Liu, X.; Tok, A. I. Y.; Lipik, V., Body temperature-responsive two-way and moisture-responsive one-way shape memory behaviors of poly(ethylene glycol)-based networks. *Polymer Chemistry* **2017**, *8*, 3833-3840.
100. Cui, Y.; Tan, M.; Zhu, A.; Guo, M., Mechanically strong and stretchable PEG-based supramolecular hydrogel with water-responsive shape-memory property. *Journal of Materials Chemistry B* **2014**, *2*, 2978-2982.
101. Wang, Y.; Cheng, Z.; Liu, Z.; Kang, H.; Liu, Y., Cellulose nanofibers/polyurethane shape memory composites with fast water-responsivity. *Journal of Materials Chemistry B* **2018**, *6*, 1668-1677.
102. Fang, Z.; Kuang, Y.; Zhou, P.; Ming, S.; Zhu, P.; Liu, Y.; Ning, H.; Chen, G., Programmable Shape Recovery Process of Water-Responsive Shape-Memory Poly(vinyl alcohol) by Wettability Contrast Strategy. *ACS Applied Materials & Interfaces* **2017**, *9*, 5495-5502.
103. Chen, H.; Li, Y.; Tao, G.; Wang, L.; Zhou, S., Thermo- and water-induced shape memory poly(vinyl alcohol) supramolecular networks crosslinked by self-complementary quadruple hydrogen bonding. *Polymer Chemistry* **2016**, *7*, 6637-6644.
104. Wang, W.; Lu, H.; Liu, Y.; Leng, J., Sodium dodecyl sulfate/epoxy composite: water-induced shape memory effect and its mechanism. *Journal of Materials Chemistry A* **2014**, *2*, 5441-5449.
105. Zhang, Y.; Zhou, S.; Zhang, L.; Yan, Q.; Mao, L.; Wu, Y.; Huang, W., Pre-Stretched Double Network Polymer Films Based on Agarose and Polyacrylamide with Sensitive Humidity-Responsive Deformation, Shape Memory, and Self-Healing Properties. *Macromolecular Chemistry and Physics* **2020**, *221*, 1900518.
106. Wong, W. S. Y.; Li, M.; Nisbet, D. R.; Craig, V. S. J.; Wang, Z.; Tricoli, A., Mimosa Origami: A nanostructure-enabled directional self-organization regime of materials. *Science Advances* **2016**, *2*.
107. Chen, Q.; Qian, X.; Xu, Y.; Yang, Y.; Wei, Y.; Ji, Y., Harnessing the Day-Night Rhythm of Humidity and Sunlight into Mechanical Work Using Recyclable and Reprogrammable Soft Actuators. *ACS Applied Materials & Interfaces* **2019**, *11*, 29290-29297.
108. Lee, S.-W.; Prosser, J. H.; Purohit, P. K.; Lee, D., Bioinspired Hygromorphic Actuator Exhibiting Controlled Locomotion. *ACS Macro Letters* **2013**, *2*, 960-965.
109. Lunni, D.; Cianchetti, M.; Filippeschi, C.; Sinibaldi, E.; Mazzolai, B., Plant-Inspired Soft Bistable Structures Based on Hygroscopic Electrospun Nanofibers. *Advanced Materials Interfaces* **2020**, *1901310*.
110. Tu, Y.; Yuan, J.; Lei, D.; Tan, H.; Wei, J.; Huang, W.; Zhang, L., TiO<sub>2</sub>-pattern-modulated actuation of an agarose@CNT/agarose bilayer induced by light and humidity. *Journal of Materials Chemistry A* **2018**, *6*, 8238-8243.
111. Andres, C. M.; Zhu, J.; Shyu, T.; Flynn, C.; Kotov, N. A., Shape-Morphing Nanocomposite Origami. *Langmuir* **2014**, *30*, 5378-5385.
112. Liang, S.; Qiu, X.; Yuan, J.; Huang, W.; Du, X.; Zhang, L., Multiresponsive Kinematics and Robotics of Surface-Patterned



- Polymer Film. *ACS Applied Materials & Interfaces* **2018**, *10*, 19123-19132.
113. Ryabchun, A.; Lancia, F.; Nguindjel, A.-D.; Katsonis, N., Humidity-responsive actuators from integrating liquid crystal networks in an orienting scaffold. *Soft Matter* **2017**, *13*, 8070-8075.
114. Haan, L. T. d.; Verjans, J. M. N.; Broer, D. J.; Bastiaansen, C. W. M.; Schenning, A. P. H. J., Humidity-Responsive Liquid Crystalline Polymer Actuators with an Asymmetry in the Molecular Trigger That Bend, Fold, and Curl. *Journal of the American Chemical Society* **2014**, *136*, 10585-10588.
115. Verpaalen, R. C. P.; Debije, M. G.; Bastiaansen, C. W. M.; Halilović, H.; Engels, T. A. P.; Schenning, A. P. H. J., Programmable helical twisting in oriented humidity-responsive bilayer films generated by spray-coating of a chiral nematic liquid crystal. *Journal of Materials Chemistry A* **2018**, *6*, 17724-17729.
116. Echeverria, C.; Aguirre, L. E.; Merino, E. G.; Almeida, P. L.; Godinho, M. H., Carbon Nanotubes as Reinforcement of Cellulose Liquid Crystalline Responsive Networks. *ACS Applied Materials & Interfaces* **2015**, *7*, 21005-21009.
117. Wu, T.; Li, J.; Li, J.; Ye, S.; Wei, J.; Guo, J., A bio-inspired cellulose nanocrystal-based nanocomposite photonic film with hyper-reflection and humidity-responsive actuator properties. *Journal of Materials Chemistry C* **2016**, *4*, 9687-9696.
118. Carter, N. A.; Grove, T. Z., Protein Self-Assemblies That Can Generate, Hold, and Discharge Electric Potential in Response to Changes in Relative Humidity. *Journal of the American Chemical Society* **2018**, *140*, 7144-7151.
119. Kim, S. H.; Kwon, C. H.; Park, K.; Mun, T. J.; Lepró, X.; Baughman, R. H.; Spinks, G. M.; Kim, S. J., Bio-inspired, Moisture-Powered Hybrid Carbon Nanotube Yarn Muscles. *Scientific Report* **2016**, *6*, 23016.
120. Li, H.; Wang, J., Ultrafast yet Controllable Dual-Responsive All-Carbon Actuators for Implementing Unusual Mechanical Movements. *ACS Applied Materials & Interfaces* **2019**, *11*, 10218-10225.
121. Kang, H.; Lee, M.; Lim, H.; Stone, H. A.; Lee, J., Hygromorphic actuator from a metal oxide film driven by a nano-capillary forest structure. *NPG Asia Materials* **2017**, *9*, e417.
122. Huang, Y.; Liang, J.; Chen, Y., The application of graphene based materials for actuators. *Journal of Materials Chemistry* **2012**, *22*, 3671-3679.
123. Baughman, R. H.; Cui, C.; Zakhidov, A. A.; Iqbal, Z.; Barisci, J. N.; Spinks, G. M.; Wallace, G. G.; Mazzoldi, A.; Rossi, D. D.; Rinzler, A. G.; Jaszinski, O.; Roth, S.; Kertesz, M., Carbon Nanotube Actuators. *Science* **1999**, *284*, 1340-1344.
124. Cheng, H.; Hu, Y.; Zhao, F.; Dong, Z.; Wang, Y.; Chen, N.; Zhang, Z.; Qu, L., Moisture-Activated Torsional Graphene-Fiber Motor. *Adv Mater* **2014**, *26*, 2909-2913.
125. He, J.; Xiao, P.; Zhang, J.; Liu, Z.; Wang, W.; Qu, L.; Ouyang, Q.; Wang, X.; Chen, Y.; Chen, T., Highly Efficient Actuator of Graphene/Polydopamine Uniform Composite Thin Film Driven by Moisture Gradient. *Advanced Materials Interfaces* **2016**, *3*, 1600169.
126. Zhang, Y.-L.; Liu, Y.-Q.; Han, D.-D.; Ma, J.-N.; Wang, D.; Li, X.-B.; Sun, H.-B., Quantum-Confined-Superfluidics-Enabled Moisture Actuation Based on Unilaterally Structured Graphene Oxide Papers. *Adv Mater* **2019**, *31*, 1901585.
127. Ge, Y.; Cao, R.; Ye, S.; Chen, Z.; Zhu, Z.; Tu, Y.; Ge, D.; Yang, X., A bio-inspired homogeneous graphene oxide actuator driven by moisture gradients. *Chemical Communications* **2018**, *54*, 3126-3129.
128. Xu, G.; Chen, J.; Zhang, M.; Shi, G., An ultrasensitive moisture driven actuator based on small flakes of graphene oxide. *Sensors and Actuators B: Chemical* **2017**, *242*, 418-422.
129. Han, D.-D.; Zhang, Y.-L.; Jiang, H.-B.; Xia, H.; Feng, J.; Chen, Q.-D.; Xu, H.-L.; Sun, H.-B., Moisture-Responsive Graphene Paper Prepared by Self-Controlled Photoreduction. *Adv Mater* **2015**, *27*, 332-338.
130. Xu, G.; Zhang, M.; Zhou, Q.; Chen, H.; Gao, T.; Li, C.; Shi, G., A small graphene oxide sheet/polyvinylidene fluoride bilayer actuator with large and rapid responses to multiple stimuli. *Nanoscale* **2017**, *9*, 17465-17470.
131. Wang, W.; Xiang, C.; Zhu, Q.; Zhong, W.; Li, Mufang; Yan, K.; Wang, D., Multistimulus Responsive Actuator with GO and Carbon Nanotube/PDMS Bilayer Structure for Flexible and Smart Devices. *ACS Applied Materials & Interfaces* **2018**, *10*, 27215-27223.
132. Dong, Y.; Wang, J.; Guo, X.; Yang, S.; Ozen, M. O.; Chen, P.; Liu, X.; Du, W.; Xiao, F.; Demirci, U.; Liu, B.-F., Multi-stimuli-programmable biomimetic actuator. *Nature Communications* **2019**, *10*, 4087.
133. Li, J.; Mou, L.; Zhang, R.; Sun, J.; Wang, R.; An, B.; Chen, H.; Inoue, K.; Ovalle-Robles, R.; Liu, Z., Multi-responsive and multi-motion bimorph actuator based on super-aligned carbon nanotube sheets. *Carbon* **2019**, *148*, 487-495.
134. Chen, H.; Ge, Y.; Ye, S.; Zhu, Z.; Tu, Y.; Ge, D.; Xu, Z.; Chen, W.; Yang, X., Water transport facilitated by carbon nanotubes enables a hygroresponsive actuator with negative hydrotaxis. *Nanoscale* **2020**, *12*, 6104-6110.
135. Lee, M.; Han, G.; Lee, J., Humidity responsive single-layered film fabricated by hydrophilic titanium oxide nanotubes. *Applied Physics Letters* **2019**, *115*, 091601.
136. Boudot, M.; Elettro, H.; Grosso, D., Converting Water Adsorption and Capillary Condensation in Usable Forces with Simple Porous Inorganic Thin Films. *ACS Nano* **2016**, *10*, 10031-10040.
137. Ye, X.-L.; Liu, L.-Z.; Jin, H.-J., Responsive nanoporous metals: recoverable modulations on strength and shape by watering. *Nanotechnology* **2016**, *27*, 325501.
138. Ma, M.; Bétard, A. I.; Weber, I.; Al-Hokbany, N. S.; Fischer, R. A.; Metzler-Nolte, N., Iron-Based Metal–Organic Frameworks MIL-88B and NH<sub>2</sub>-MIL-88B: High Quality Microwave Synthesis and Solvent-Induced Lattice “Breathing”. *Crystal Growth & Design* **2013**, *13*, 2286-2291.
139. Troyano, J.; Carne-Sanchez, A.; Perez-Carvajal, J.; Leln-Reina, L.; Imaz, I.; Cabeza, A.; Maspoch, D., A Self-Folding Polymer Film Based on Swelling Metal–Organic Frameworks. *Angewandte Chemie International Edition* **2018**, *130*, 15646-15650.
140. Troyano, J.; Carné-Sánchez, A.; Maspoch, D., Programmable Self-Assembling 3D Architectures Generated by Patterning of Swellable MOF-Based Composite Films. *Adv Mater* **2019**, *31*, 1808235.
141. Virta, J.; Koponen, S.; Absetz, I., Measurement of swelling stresses in spruce (*Picea abies*) samples. *Building and Environment* **2006**, *41*, 1014-1018.
142. Masic, A.; Bertinetti, L.; Schuetz, R.; Chang, S.-W.; Metzger, T. H.; Buehler, M. J.; Fratzl, P., Osmotic pressure induced tensile forces in tendon collagen. *Nature Communications* **2015**, *6*, 5942.
143. Cakmak, O.; Tinay, H. O. E.; Chen, X.; Sahin, O., Spore-Based Water-Resistant Water-Responsive Actuators with High Power Density. *Advanced Materials Technologies* **2019**, 1800596.
144. Roh, S.; Parekh, D. P.; Bharti, B.; Stoyanov, S. D.; Velev, O. D., 3D Printing by Multiphase Silicone/Water Capillary Inks. *Adv Mater* **2017**, *29*, 10.1002/adma.201701554.
145. Wang, W.; Xiang, C.; Liu, Q.; Li, M.; Zhong, W. Z.; Yana, K.; Wang, D., Natural alginate fiber-based actuator driven by water or moisture for energy harvesting and smart controller applications. *Journal of Materials Chemistry A* **2018**, *6*, 22599-22608.

146. Zhou, P.; Chen, L.; Yao, L.; Weng, M.; Zhang, W., Humidity- and light-driven actuators based on carbon nanotube-coated paper and polymer composite. *Nanoscale* **2018**, *10*, 8422-8427.
147. Gao, L.; Guo, G.; Liu, M.; Tang, Z.; Xie, L.; Huo, Y., Multi-responsive, bidirectional, and large deformation bending actuators based on borax cross-linked polyvinyl alcohol derivative hydrogel. *RSC Advances* **2017**, *7*, 40005-40014.
148. Deng, H.; Zhang, C.; Su, J.-W.; Xie, Y.; Zhang, C.; Lin, J., Bioinspired multi-responsive soft actuators controlled by laser tailored graphene structures. *Journal of Materials Chemistry B* **2018**, *6*, 5415-5423.
149. Zhao, Z.; Kuang, X.; Yuan, C.; Qi, H. J.; Fang, D., Hydrophilic/Hydrophobic Composite Shape-Shifting Structures. *ACS Applied Materials & Interfaces* **2018**, *10*, 19932-19939.
150. Mulakkal, M. C.; Trask, R. S.; Ting, V. P.; Seddon, A. M., Responsive cellulose-hydrogel composite ink for 4D printing. *Materials and Design* **2018**, *160*, 108-118.
151. Wang, W.; Xiang, C.; Sun, D.; Li, M.; Yan, K.; Wang, D., Photothermal and Moisture Actuator Made with Graphene Oxide and Sodium Alginate for Remotely Controllable and Programmable Intelligent Devices. *ACS Applied Materials & Interfaces* **2019**, *11*, 21926-21934.
152. Dai, M.; Picot, O. T.; Verjans, J. M. N.; Haan, L. T. d.; Schenning, A. P. H. J.; Peijs, T.; Bastiaansen, C. W. M., Humidity-Responsive Bilayer Actuators Based on a Liquid-Crystalline Polymer Network. *ACS Applied Materials & Interfaces* **2013**, *5*, 4945-4950.
153. Roh, S.; Okello, L. B.; Golbasi, N.; Hankwitz, J. P.; Liu, J. A. C.; Tracy, J. B.; Velev, O. D., 3D-Printed Silicone Soft Architectures with Programmed Magneto-Capillary Reconfiguration. *Advanced Materials Technologies* **2019**, *4*.
154. Chen, Q.; Yan, X.; Lu, H.; Zhang, N.; Ma, M., Programmable Polymer Actuators Perform Continuous Helical Motions Driven by Moisture. *ACS Applied Materials & Interfaces* **2019**, *11*, 20473-20481.

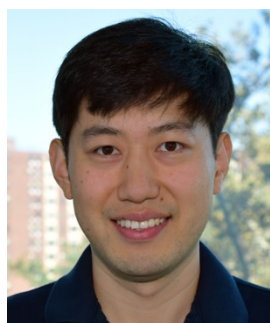
## Table of Contents



Up-to-date studies of water-responsive materials for energy-related applications are reviewed. Future research endeavours could advance scientific and technical challenges.



Yaewon Park received her B.S. and M.S. in Textile Science from Seoul National University, South Korea and her Ph.D. in Fiber and Polymer Science from North Carolina State University. She is currently a postdoctoral research associate at the Advanced Science Research Center of the City University of New York. Her research interests include stimuli-responsive polymers and fibres, functionalization of textile fibres by incorporating biological matters and biomimetic design for protective applications.



Xi Chen is an Assistant Professor in the Nanoscience Initiative at the CUNY Advanced Science Research Center and the Department of Chemical Engineering at the City College of New York. Prior to his appointment, he was a postdoctoral fellow in Biological Sciences at Columbia University. He earned his Ph.D. in Mechanical Engineering from Stevens Institute of Technology after receiving his B.S. and M.S. degrees from Tsinghua University. His current research focuses on identifying the fundamental mechanisms behind materials' water-responsive (WR) behaviours, scaling up nanoscale WR materials into actuators or artificial muscles, and developing WR materials based actuators and energy harvesting devices.